

Copper(II) Complexes of Aminocarbohydrate β -Ketoenaminic Ligands: Efficient Catalysts in Catechol Oxidation

Rainer Wegner,^[a] Michael Gottschaldt,^[b] Helmar Görls,^[a]
Ernst-G. Jäger,^{*[a]} and Dieter Klemm^{*[b]}

Dedicated to Prof. Dr. Dieter Sellmann on the occasion of his 60th birthday

Abstract: Copper(II) complexes of tridentate dianionic β -ketoenaminic ligands derived from differently functionalized amino-deoxyglucoses were synthesized and characterized with respect to their structural, spectroscopic, and catalytic properties. The (probably dimeric) complex {1,2-*O*-isopropylidene-6-*N*-(3-acetyl-2-oxobut-3-enyl)amino-6-deoxyglucofuranosyl}copper(II) Cu(**3a**) was a highly efficient catalyst for the catechol-oxidase-like oxidation of 3,5-di-*tert*-butylcatechol (dtbc) into 3,5-di-*tert*-butylquinone (dtbq) by molecular oxygen ($k_{\text{cat}} = 2.63 \text{ s}^{-1}$). In contrast to this magnetically “normal” complex Cu(**3a**), the analogous dinuclear com-

plex $[\{\text{Cu}(\mathbf{2a})\}_2]$, derived from the isomeric amino sugar 5-amino-5-deoxyglucofuranose, forms six-membered chelate rings with the sugar moiety and has very strong antiferromagnetic-coupled copper atoms (resulting in a diamagnetic ground state). It has a rather insignificant activity ($k_{\text{cat}} < 10^{-3} \text{ s}^{-1}$). The ligand H₂**1a**, derived from a (protected) 6-amino-6-deoxyglucopyranose, forms a trinuclear complex $[\{\text{Cu}(\mathbf{1a})\}_2 \cdot \text{Cu}(\text{OAc})_2]$ in which two basic formula units are

bridged by one copper acetate. This compound and the complex derived from an (isomeric) aminodeoxyglucopyranose ($[\text{Cu}(\mathbf{4a})]$; $k_{\text{cat}} \approx 0.03 \text{ s}^{-1}$) show moderate activity. All complexes with a peripheral ethoxycarbonyl group instead of the acetyl substituent R², Cu(**1b**)–Cu(**3b**) and Cu(**4c**), are inactive. The complexes derived from 2-hydroxycyclohexylamine, Cu(**5a**) and Cu(**5c**), which were used as models of the active complex Cu(**3a**), have the typical “cubane-like” tetranuclear structure known from many copper complexes with derivatives of saturated 2-aminoalcohols. They are inactive with respect to the activation of dioxygen.

Keywords: carbohydrates • copper • magnetic properties • oxidation • Schiff bases

Introduction

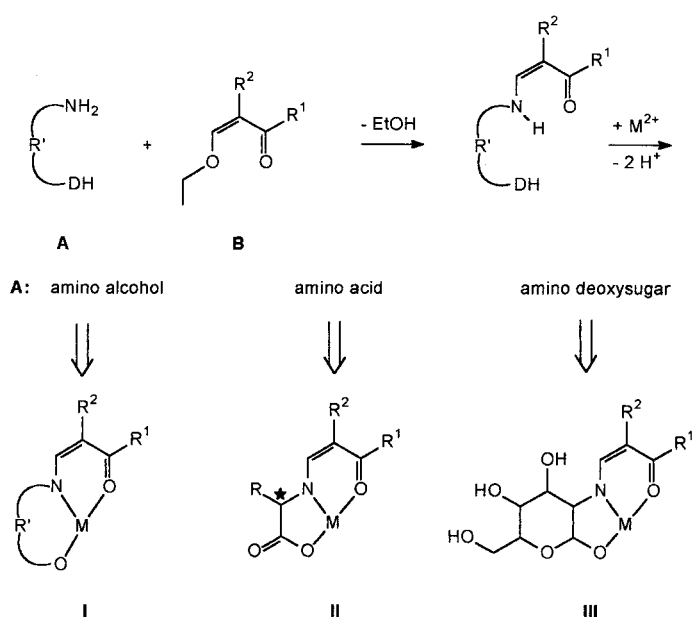
Di- and oligonuclear copper complexes represent the active site of many copper proteins involved in transport, storage, and activation of molecular oxygen. For the four-electron reduction of dioxygen, nature favors structures such as the dinuclear center in catechol oxidase^[1] or the active site of ascorbate oxidase^[2] with a trinuclear unit and an additional “type I” copper atom. Intensive studies on oligonuclear

copper model compounds have been undertaken in recent years to elucidate the relationship between structure and reactivity of the natural active sites and to develop new complexes with a useful catalytic performance.^[3–7] In most cases, dinucleating (macrocyclic or open-chain) ligands were used for the design of such complexes. In our approach (Scheme 1), we use tridentate ligands derived from condensation products of a primary amine **A**, which bears an additional donor (D), such as O, S, and R–N, with a substituted 3-oxo-enol **B** to reach coordinatively unsaturated formula units of complexes that tend to give oligonuclear structures. The substituents R¹ and R² can be used to control the electronic properties of the metal center (redox behavior, Lewis acidity),^[8] whilst the bridges R' mainly determine the structure, stability, and reactivity of the coordinatively saturated oligonuclear species.

Even the first examples of copper complexes, **I**, derived from 2-hydroxyethylamine, confirmed the high tendency of such formula units towards spontaneous oligomerization:^[9] they form very stable tetranuclear molecules with a cubane-

[a] Prof. Dr. E.-G. Jäger, Dr. R. Wegner, Dr. H. Görls
Friedrich Schiller Universität Jena
Institute of Inorganic and Analytical Chemistry
August-Bebel-Strasse 2, 07743 Jena (Germany)
Fax: (+49) 3641-948102
E-mail: cej@rz.uni-jena.de

[b] Prof. Dr. D. Klemm, Dipl.-Chem. M. Gottschaldt
Friedrich Schiller Universität Jena
Institute of Organic and Macromolecular Chemistry
Humboldtstrasse 10, 07743 Jena (Germany)
Fax: (+49) 3641-948202
E-mail: c9kldi@rz.uni-jena.de



Scheme 1. Coordinatively unsaturated formula units of metal complexes with tridentate ligand anions based on functionalized 3-oxo-1-enamines as building blocks for oligonuclear structures.

like $[\text{Cu}_4\text{O}_4]$ core^[10] and “normal” magnetic behavior ($S = 1/2$) at room temperature. Later on, it was realized that this motif is a typical structural feature of many complexes **I** with $\text{R}' = \text{CH}_2\text{-CH}_2$, whereas the derivatives of other hydroxamines (e.g., with aromatic or longer aliphatic bridges R') give mainly dinuclear species, characterized by a more or less strong magnetic coupling of the copper centers.^[11–22] Interesting di- and tetranuclear metalla-macrocycles have been isolated from copper complexes of type **II** with histidine as the amine component **A**.^[23] Their oligonuclear structures are stable even in the presence of strong additional ligands, such as pyridine or *N*-methylimidazole.

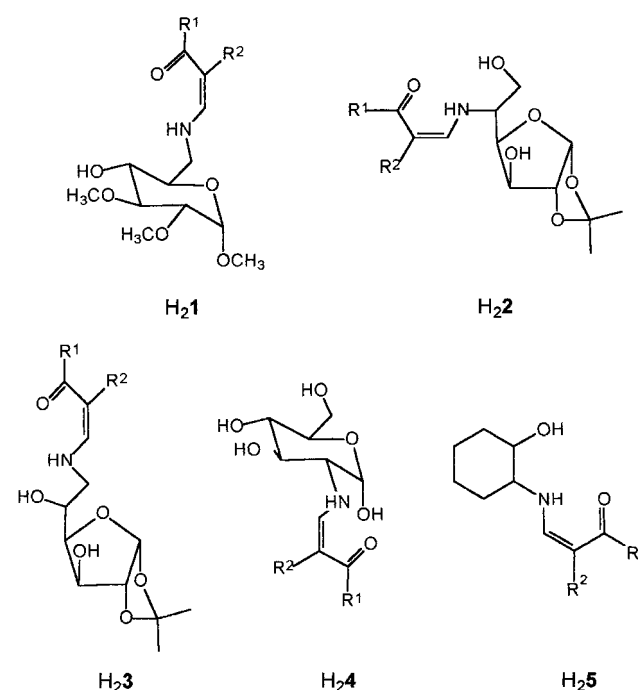
Recently, we described the first structurally characterized prototypes^[24] of complexes derived from aminodeoxysugars as amine component **A** (formula **III** presents one of a big variety of hypothetical structures of this general type of complexes). Based on current knowledge, carbohydrates are not typical ligands in biological metal complexes. However, as a backbone in synthetic “mimics” they offer valuable advantages: they are chiral, polyfunctional, natural substances that exist in a broad region of molecular size and obey unique conformational and configurative principles. They can be selectively functionalized and can have supramolecular structures (fibers, gels, membranes, mono- and multilayers)^[25–27] as mono-, oligo-, or polysaccharides. Solubility can be regulated in a wide range, as well as the biological activity, compatibility, and the possible biological decomposition. Recent studies of the organometallic^[28] and coordination chemistry^[29–34] of *N*-glycosides, nonmodified carbohydrates, and inositols have shown that carbohydrates have a very interesting potential as complex ligands.

In the case of our copper complexes with derivatives of amino sugars, we observed an interesting catalytic activity in the catechol-oxidase-like oxidation of di-*tert*-butylcatechol (dtbc) to the corresponding quinone by molecular oxygen.^[24]

This paper will give a more detailed discussion of this phenomenon, including new complexes of new amino sugar derivatives. Additionally, two complexes of type **I** with a cyclohexane-1,2-diyl bridge R' are included for comparison. This cyclic chiral bridge R' has some structural features in common with the six-membered ring of a pyranose, but without the possible effects of additional hydroxy or alkoxy substituents.

Results and Discussion

The basic structures of ligands used in this study and their abbreviations are given in Scheme 2. The ligands **H**₂**1**–**H**₂**4** are derived from aminodeoxyglucoses with a systematic



Scheme 2. Overview and abbreviations of ligands used (the type of substituents is symbolized by small bold letters **a**: $\text{R}^1 = \text{Me}$, $\text{R}^2 = \text{COMe}$, **b**: $\text{R}^1 = \text{OEt}$, $\text{R}^2 = \text{CO}_2\text{Et}$; **c**: $\text{R}^1 = \text{Me}$; $\text{R}^2 = \text{CO}_2\text{Et}$).

variation of the position of the functionalized amino group; they have at least one free hydroxyl group in the neighborhood of the amino function. Formally, they should react with copper(II) ions as derivatives of 1,2- or 1,3-aminoalcohols.^[9, 10] In the case of deprotonation of the enamine-NH in addition to one hydroxyl group, **H**₂**1** should give an additional six-membered chelate ring with the central copper atom. In the case of **H**₂**2**, either a five-membered ring (with O at the terminal C⁶ of the sugar chain) or a six-membered ring (with the O at C³) could be expected. Ligand **H**₂**3** should give a five-membered ring (with O at C⁵) or (but very improbably) a seven-membered ring (with O at C³). In the case of **H**₂**4**, many possibilities exist: five-membered rings could be formed with O at C¹ or C³, whereas six- or eight-membered rings should be possible with O at C⁴ or C⁶. The model ligands **H**₂**5** give only five-membered additional rings that strongly resemble the

pyranose derivatives **H₂4**, but with respect to the size of possible chelate rings, they are also similar to **H₂2** and **H₂3**.

The following ligands have been isolated as solids and characterized by their melting points (with exception of the oily **H₂1** and **H₂5**), elemental analysis, and ¹H NMR, ¹³C NMR, and IR spectroscopy: **H₂1a**, **H₂1b**, **H₂2a**, **H₂2b**, **H₂3a**, **H₂3b**, **H₂5a**, **H₂5c**.

The ligands **H₂4a** and **H₂4c** were formed in situ and these solutions were used to prepare the complexes directly.

Copper(II) complexes of the following compositions were isolated and have been characterized by elemental analysis, MS, UV/Vis, IR, and (in part) EPR spectra, and magnetic behavior. Although structure determinations by X-ray analysis were possible only for the complexes of **H₂1a**, **H₂2a**, **H₂5a**, and **H₂5c**, the expected tendency to spontaneous oligomerization could be proved in all cases by mass spectrometry: [[Cu(**1a**)₂·Cu(OAc)₂], [[Cu(**1b**)₂·Cu(OAc)₂], [[Cu(**2a**)₂·H₂O][Cu(**2a**)₂·MeOH] (from MeOH/water), [[Cu(**2a**)₂] (from toluene), [[Cu(**2b**)₂], [[Cu(**3a**)_x], [[Cu(**3b**)_x], [[Cu(**4a**)₂·(Et₃NH)OAc], [[Cu(**4c**)₂·(Et₃NH)OAc], [[Cu(**5a**)₄], [[Cu(**5c**)₄].

In the following, the complexes are symbolized in general by their formula unit “Cu(L)” only, independent of their correct composition. In fact, the complexes differ decisively in their structure and catalytic activity because of the specific

influence of the carbohydrate. The ligands **H₂5**, which bear a *trans*-cyclohexan-1,2-diyl bridge R' but without additional O-functional groups, give the expected solvent-free complexes with the tetranuclear structure typical for complexes with derivatives of simpler aliphatic 2-aminoalcohols.

Crystal and molecular structures: Crystals that were suitable for X-ray structure determination were obtained for compounds Cu(**1a**), Cu(**2a**), Cu(**5a**), and Cu(**5c**). The structures of the copper(II) complexes obtained with the ligands **H₂1a** and **H₂2a** have recently been presented in a preliminary communication.^[24] Details of crystal structure determination and refinement for both complexes are listed in Table 1. Table 2 gives selected bond lengths and angles as well as the nonbonding distances for the complex of **H₂1a**.

The ligand **H₂1a** reacts with copper(II) acetate in ethanol/water in the presence of triethylamine to give crystals of a trinuclear complex in which two Cu(**1a**) units are bridged by one copper(II) acetate. Figure 1 shows the stereoviews of the complete molecule (top), the arrangement of the chelate and pyranose rings (middle), and the coordination around the three copper atoms (bottom). Figure 2 shows the intermolecular bonding in the unit cell.

The unit cell contains two formula units of the trinuclear complex [[Cu(**1a**)·{Cu(OAc)₂}·{Cu(**1a**)}]. Both of the

Table 1. Crystal data of Cu(**1a**), Cu(**2a**), [[Cu(**5a**)₄], and [[Cu(**5c**)₄].

	[[Cu(1a) ₂ ·Cu(OAc) ₂]	[[Cu(2a) ₂ ·H ₂ O][Cu(2a) ₂ ·MeOH]	[[Cu(5c) ₄]	[[Cu(5a) ₄]
formula	C ₃₄ H ₅₂ N ₂ O ₁₈ Cu ₃	C ₃₀ H ₄₂ Cu ₂ N ₂ O ₁₄ ·1.75 H ₂ O·0.5 CH ₃ OH	C ₅₂ H ₇₆ N ₄ O ₁₆ Cu ₄	C ₄₈ H ₆₈ N ₄ O ₁₂ Cu ₄
<i>M_r</i> [g mol ⁻¹]	967.40	837.79	1267.37	1147.27
crystal size [mm]	0.32 × 0.30 × 0.20	0.28 × 0.24 × 0.20	0.32 × 0.30 × 0.20	0.32 × 0.28 × 0.22
shape	blue prisms	blue prisms	blue prisms	blue prisms
crystal system	monoclinic	monoclinic	triclinic	monoclinic
space group	<i>P</i> 2 ₁ (No. 4)	<i>P</i> 2 ₁ (No. 4)	<i>P</i> 1̄ (No. 2)	<i>P</i> 2 ₁ / <i>c</i> (No. 14)
<i>a</i> [Å]	10.0735(3)	10.3923(3)	11.0027(3)	15.204(1)
<i>b</i> [Å]	21.3865(7)	13.8859(5)	14.5085(5)	17.648(1)
<i>c</i> [Å]	10.4135(2)	25.9903(8)	20.8019(9)	22.137(8)
α [°]			72.647(2)	90
β [°]	110.789(1)	101.517(2)	76.552(2)	93.706(3)
γ [°]			71.707(2)	90
<i>V</i> [Å ³]	2097.4(1)	3675.1(2)	2973.77(18)	5927(2)
<i>T</i> [°C]	-90	-90	-90	20
<i>Z</i>	2	4	2	4
ρ_{calcd} [g cm ⁻³]	1.532	1.514	1.415	1.286
μ (MoK α) [cm ⁻¹]	15.82	12.33	14.77	14.7
<i>F</i> (000)	1002	1748	1320	2384
reflections measured	6973	15126	20079	19348
index ranges	-12 ≤ <i>h</i> ≤ 12 -20 ≤ <i>k</i> ≤ 26 -12 ≤ <i>l</i> ≤ 13	0 ≤ <i>h</i> ≤ 14 -19 ≤ <i>k</i> ≤ 19 -25 ≤ <i>l</i> ≤ 27	0 ≤ <i>h</i> ≤ 13 -16 ≤ <i>k</i> ≤ 18 -24 ≤ <i>l</i> ≤ 25	-18 ≤ <i>h</i> ≤ 18 -19 ≤ <i>k</i> ≤ 22 -27 ≤ <i>l</i> ≤ 27
θ range [°]	5.19 ≤ θ ≤ 26.37	2.30 ≤ θ ≤ 30.52	3.17 ≤ θ ≤ 26.40	3.29 ≤ θ ≤ 26.44
independent reflections	6973	14812	12079	11928
observed reflections ^[a]	6127	11657	7830	5646
parameters	514	933	722	613
restraints	1	1	0	0
<i>R</i> ¹ _{obs}	0.039	0.081	0.060	0.087
<i>wR</i> ² _{obs}	0.087	0.141	0.106	0.211
<i>R</i> ¹ _{all}	0.050	0.1106	0.114	0.196
<i>wR</i> ² _{all}	0.094	0.1533	0.124	0.260
goodness of fit	1.029	1.095	1.004	0.983
Flack parameter <i>x</i>	0.01(1)	0.35(1)	0	0
highest peak [e Å ⁻³]	0.257	0.646	0.570	1.340
deepest hole [e Å ⁻³]	-0.355	-0.695	-0.613	-0.520

[a] *F*₀ > 4σ(*F*₀).

Table 2. Selected interatomic distances, and bond lengths [Å] and angles [°] in $[\text{Cu}(\mathbf{1a})_2 \cdot \text{Cu}(\text{OAc})_2]$.

Cua...Cub	5.735(3)	Cua...Cuc	3.248(3)
Cub...Cuc	3.207(3)		
Cua-O1a	1.911(3)	Cua-O7a	1.921(3)
Cua-N1a	1.954(3)	Cua-O8a	1.968(3)
Cua...O6b ^[a]	2.753(3)	Cub-O1b	1.898(3)
Cub-O7b	1.913(3)	Cub-N1b	1.954(3)
Cub-O8b	1.962(3)	Cub...O2a	2.898(3)
Cuc-O1a	1.949(3)	Cub-O9a	1.942(3)
Cuc-O1b	1.952(3)	Cuc-O9b	1.954(3)
Cuc-O2a	2.586(3)	Cuc-O2b	2.572(3)
O1a-Cua-N1a	95.6(1)	O1a-Cua-O7a	160.7(1)
O1a-Cua...O6b ^[a]	106.9(1)	O1a-Cua-O8a	91.0(1)
O7a-Cua-O8a	86.2(1)	O7a-Cua-N1a	91.4(1)
N1a-Cua-O8a	166.4(1)	O7a-Cua...O8b ^[a]	92.0(1)
O8a-Cua...O6b ^[a]	87.4(1)	N1a-Cua...O8b ^[a]	79.3(1)
O1b-Cub-N1b	96.4(1)	O1b-Cub-O7b	164.7(1)
O1b-Cub...O2a	78.7(1)	O1b-Cub-O8b	91.2(1)
O7b-Cub-O8b	85.9(1)	O7b-Cub-N1b	92.1(1)
N1b-Cub-O8b	156.2(1)	O7b-Cub...O2a	86.1(1)
O8b-Cub...O2a	84.1(1)	N1b-Cub...O2a	119.5(1)
O1a-Cuc-O1b	94.6(1)	O1a-Cuc-O9a	90.7(1)
O1a-Cuc-O2a	73.8(1)	O1a-Cuc-O9b	171.2(1)
O9a-Cuc-O1b	172.3(1)	O1a-Cuc-O2b	88.3(1)
O9a-Cuc-O2a	100.8(1)	O9a-Cuc-O9b	85.4(1)
O1b-Cuc-O9b	90.2(1)	O9a-Cuc-O2b	100.8(1)
O1b-Cuc-O2b	73.6(1)	O1b-Cuc-O2a	86.3(1)
O9b-Cuc-O2b	100.2(1)	O9b-Cuc-O2a	99.2(1)
O2a-Cuc-O2b	152.0(1)		

[a] Symmetry operation for equivalent atoms: $-x, 0.5+y, -z$.

“outer” copper atoms, Cua and Cub, have a distorted square-pyramidal 4+1 coordination. The base plane is formed by the tridentate dianionic ligand, which gives two six-membered chelate rings (bond lengths Cua-O/N/O: 191/195/192 pm; Cub-O/N/O: 190/195/191 pm), and one O of an acetate (Cu-O: 196 pm). The apical coordination site of Cua is occupied by the peripheral acetyl oxygen atom of the neighboring molecule (O6b); bond length 275 pm). This results in chains of molecules (Figure 2). The copper atom is displaced out of the base plane by 4.6 pm towards the O6b of the next molecule. The fifth coordination site of Cub is occupied by the methoxy oxygen atom in the 3-position of the ligand molecule A (Cub-O2a: 290 pm). A similar, but weaker interaction between Cua and O2b (306 pm) results in a strongly distorted octahedral 4+1+1 coordination of Cua. The central copper atom Cuc is bound in the plane to one O of each acetate (Cu-O9: 195 pm) and to both of the coordinated alkoxide oxygens of the chelate ligands, which act as bridging donors (Cu-O1a,b: 195 pm). A weaker interaction with the 3-methoxy oxygen atoms of both pyranose units, O2a and O2b, completes the six-coordination of a distorted octahedron (Cu-O bond lengths: 259 and 257 pm, respectively). Compared to simple amino alcohol ligands, the additional donor atoms evidently cause a rare type of oligomerization in which an additional copper acetate is inserted between two building blocks of type **I**.

One striking point of this structure is the low symmetry. All copper atoms have different axial ligands and different geometric properties. The distances between the “middle” and the “outer” copper atoms differ: 325 and 321 pm,

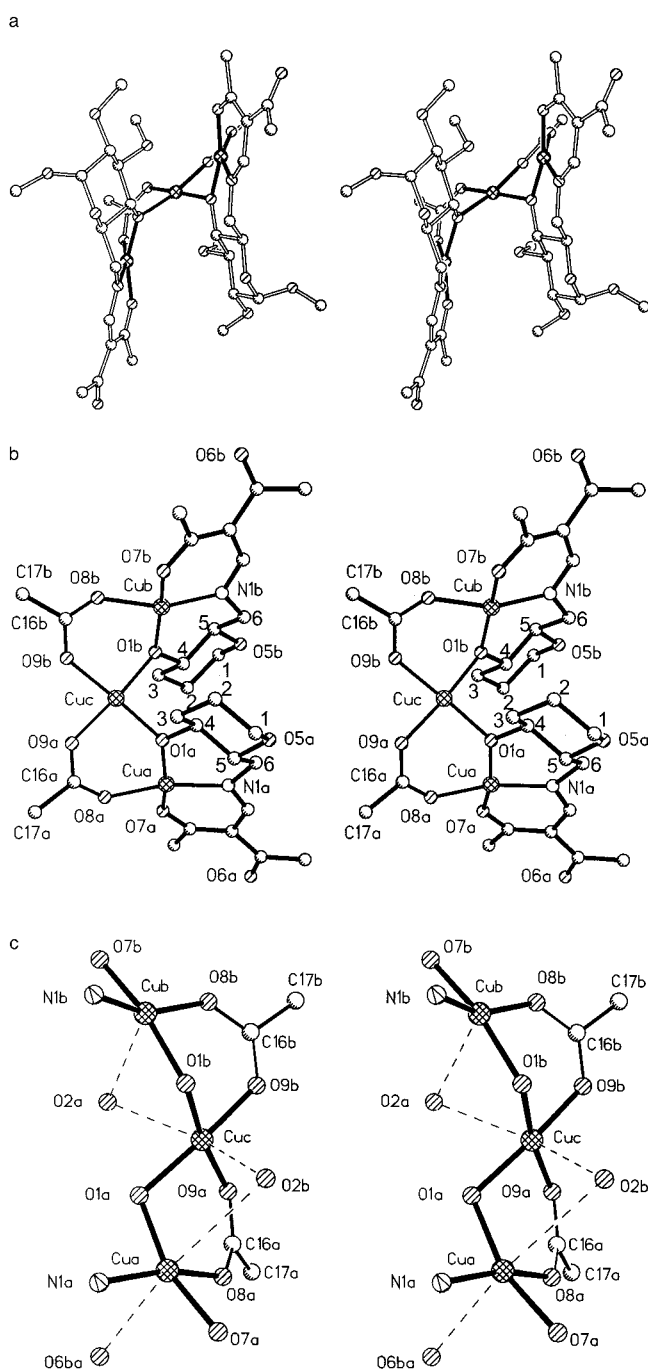


Figure 1. Stereoviews of the structure of $[\text{Cu}(\mathbf{1a})_2 \cdot \text{Cu}(\text{OAc})_2]$, a) complete trinuclear structure, b) arrangement of chelate and pyranose rings (the single Arabic numbers denote the C atoms of the glucose), c) coordination mode of the copper atoms.

respectively. These distances are very close to the mean value from the bridging of two copper atoms by a doubly deprotonated catechol, so that this seems to provide model character for catechol oxidase.

The reaction of ligand **H₂2a** with copper acetate, under the same conditions as mentioned above, gives crystals that consist of two different dinuclear formula units, $[\text{Cu}(\mathbf{2a})_2 \cdot \text{H}_2\text{O}]$ (Figure 3a) and $[\text{Cu}(\mathbf{2a})_2 \cdot \text{MeOH}]$ (Figure 3b). Selected bonding and non-bonding distances and bond angles

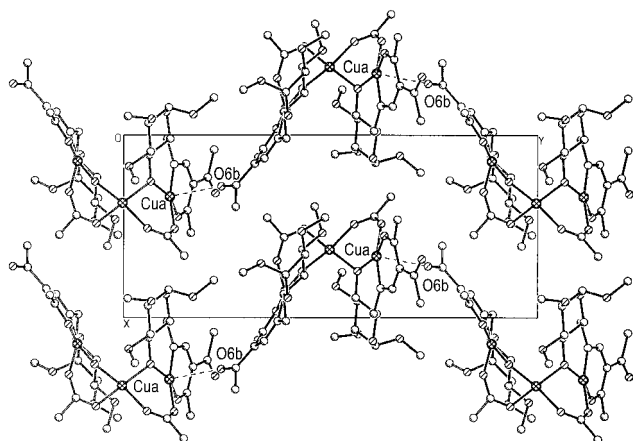


Figure 2. Unit cell and intermolecular coordination of $[[\text{Cu}(\mathbf{1a})_2]_2 \cdot \text{Cu}(\text{OAc})_2]$.

are given in Table 3, and possible hydrogen bond lengths in Table 4.

The Flack parameter of the structure determination shows that the crystal is a racemic twin. The unit cell (Figure 4) contains two formula units. Each consist of both dinuclear complexes and three additional water molecules, of which one position is only half occupied. Both dinuclear complex units are formed by dimerization of two subunits of type **I**. The alcoholate oxygen atoms in the 3-position (O2a,b and O2c,d) and the copper atoms form a central four-membered Cu_2O_2 ring with low Cu–Cu distances (298 and 302 pm, respectively). This is reminiscent of the structural motifs in catechol oxidase.^[1]

Striking is the low symmetry and high distortion of the compound. The deviation between the inner main planes of both dinuclear units is clearly shown by the fit in Figure 5. Both complexes contain one four- and one five-coordinated copper atom; the latter carries a solvent molecule (water or

Table 3. Selected interatomic distances, and bond lengths [Å] and angles [°] in $[[\text{Cu}(\mathbf{2a})_2]_2 \cdot \text{H}_2\text{O}]$ and $[[\text{Cu}(\mathbf{2a})_2]_2 \cdot \text{MeOH}]$.

Cua...Cub	2.977(1)	Cua–O1a	1.893(5)
Cua–O2a	1.930(4)	Cua–N1a	1.934(5)
Cua–O2b	1.956(4)	Cua–O8a	2.382(5)
Cub–O1b	1.902(5)	Cub–O2b	1.891(5)
Cub–N1b	1.923(5)	Cub–O2a	1.933(4)
O1a–Cua–O2a	166.6(2)	O1a–Cua–N1a	93.2(2)
O1a–Cua–O2b	91.7(2)	O1a–Cua–O8a	92.2(2)
O2a–Cua–N1a	98.0(2)	O2a–Cua–O2b	76.1(2)
O2a–Cua–O8a	92.7(2)	N1a–Cua–O2b	169.5(2)
N1a–Cua–O8a	102.1(2)	O2b–Cua–O8a	86.9(2)
O1b–Cub–O2b	167.4(2)	O1b–Cub–N1b	91.9(2)
O1b–Cub–O2a	92.3(2)	O2b–Cub–N1b	98.8(2)
O2b–Cub–O2a	77.6(2)	N1b–Cub–O2a	173.8(2)
Cua–O2a–Cub	100.8(2)	Cua–O2a–Cub	101.4(2)
Cuc...Cud	3.020(1)	Cuc–O1c	1.917(5)
Cuc–O2c	1.911(5)	Cuc–N1c	1.923(5)
Cuc–O2d	1.966(4)	Cuc–O4	2.674(5)
Cud–O1d	1.892(5)	Cud–O2d	1.922(4)
Cud–N1d	1.903(5)	Cud–O2c	1.910(5)
O1c–Cuc–O2c	171.8(2)	O1c–Cuc–N1c	92.8(2)
O1c–Cuc–O2d	95.9(2)	O1c–Cuc–O4	85.6(2)
O2c–Cuc–N1c	95.4(2)	O2c–Cuc–O2d	75.9(2)
O2c–Cuc–O4	96.4(2)	N1c–Cuc–O2d	168.5(2)
N1c–Cuc–O3	80.6(2)	O2d–Cuc–O4	107.6(2)
O1d–Cud–O2d	166.7(2)	O1d–Cud–N1d	93.6(2)
O1d–Cud–O2c	89.7(2)	O2d–Cud–N1d	99.7(2)
O2d–Cud–O2c	77.0(2)	N1d–Cud–O2c	176.1(2)
Cuc–O2c–Cud	104.5(2)	Cuc–O2d–Cud	101.9(2)

methanol) as an additional axial ligand. The four-coordinated copper atoms Cub and Cud are out of the coordination NO_3 plane by only 1.8 and 1.0 pm, respectively, and show less distortion from a strong square-planar arrangement than the five-coordinated copper atoms Cua and Cuc which are displaced by 13.1 and 6.5 pm, respectively, in direction of their axial ligands. The axial methanol at Cuc is orientated in the same direction as the furanose rings of the sugar (Figure 3b), whereas the water at Cua occupies the opposite coordination site (Figure 3a). This is caused by H bridges between the axial MeOH and the oxygen of the furanose ring in the former case (O4–O5c: 290 pm) and between the axial H_2O and the terminal 6-hydroxy group of the sugar in the latter (O8a–O4a: 283 pm). Whereas this 6-hydroxy group in the latter complex is rotated towards the solvent ligand (Figure 3a), the corresponding terminal group (O4c) in the “methanol” complex is rotated towards the periphery (Figure 3b) to permit intermolecular hydrogen bonding with the carbonyl oxygen atom O3 of the next molecule of the same species.

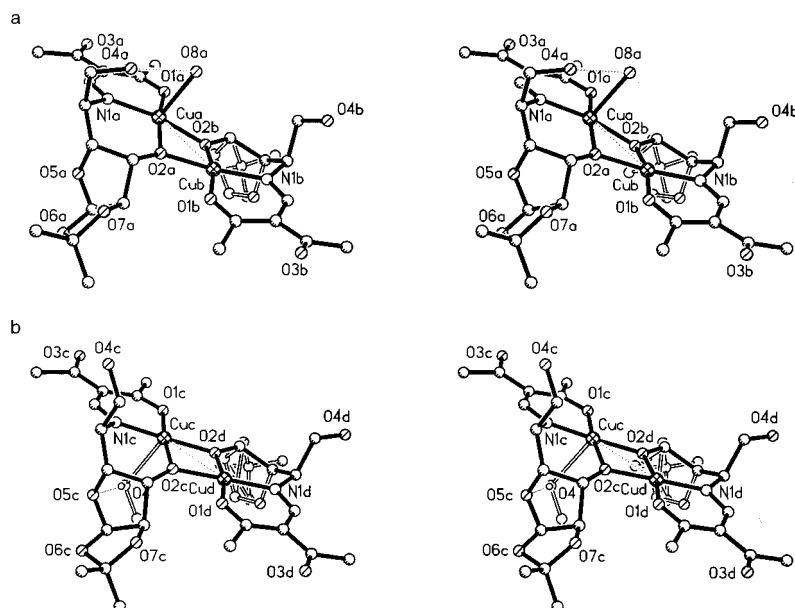
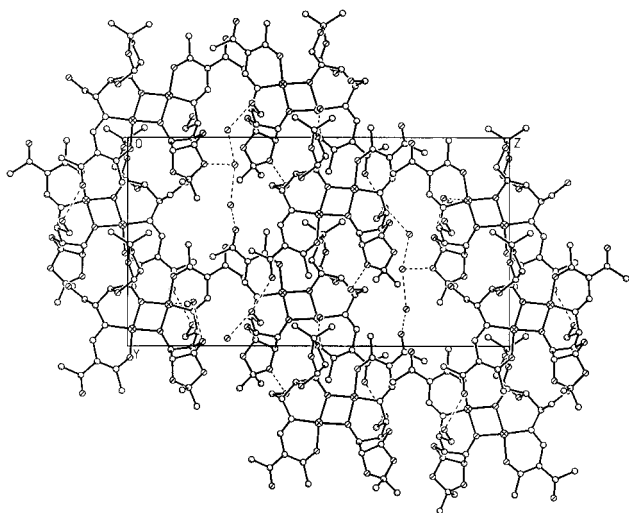
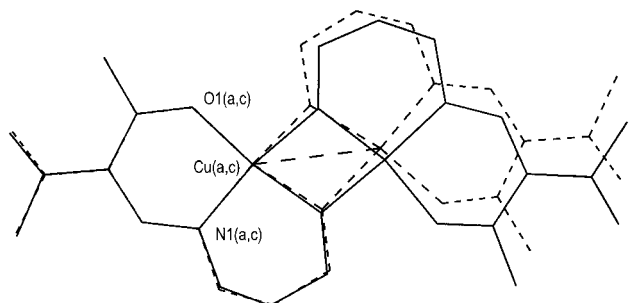


Figure 3. Stereoview of the structures of the dinuclear units a) $[[\text{Cu}(\mathbf{2a})_2]_2(\text{H}_2\text{O})]$ and b) $[[\text{Cu}(\mathbf{2a})_2]_2(\text{MeOH})]$ in the copper complex of $\text{H}_2\mathbf{2a}$.

Table 4. Hydrogen bonds in $[[\text{Cu}(\mathbf{2a})]_2 \cdot \text{H}_2\text{O}][[\text{Cu}(\mathbf{2a})]_2 \cdot \text{MeOH}]$.

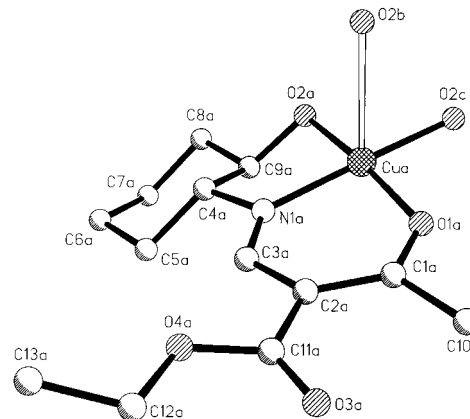
Hydrogen bond	O...O [Å]
O1-H...O3 ^[a]	2.801(2)
O2-H...O1 ^[b]	2.771(2)
O2-H...O3 ^[c]	2.961(2)
O3-H...O5	2.712(2)
O3-H...O6 ^c	2.856(2)
O4-H...O5 ^c	2.903(2)
O4a-H...O8a	2.831(2)
O8a-H...O7a ^[b]	2.875(2)
O8a-H...O2b	3.000(2)
O4b-H...O3a ^[b]	2.724(2)
O4c-H...O3d ^[d]	2.754(2)

Symmetry operations for equivalent atoms: [a] $x, y-1, z$; [b] $-x-1, y-0.5, -z-1$; [c] $-x, y+0.5, -z$; [d] $-x, y-0.5, -z$.

Figure 4. Unit cell of $[[\text{Cu}(\mathbf{2a})]_2(\text{H}_2\text{O})][[\text{Cu}(\mathbf{2a})]_2(\text{MeOH})]$.Figure 5. Superposition of the main planes of the dinuclear chelate framework of $[[\text{Cu}(\mathbf{2a})]_2(\text{H}_2\text{O})]$ (—) and $[[\text{Cu}(\mathbf{2a})]_2(\text{MeOH})]$ (---), fitted with the marked atoms.

A closer look at the unit cell (Figure 4) shows a network of additional hydrogen bonds established by the solvent molecules in the cell. All in all, this complicated network of H bridges in $\text{Cu}(\mathbf{2a})$ evidently stabilizes the low symmetry of this complex. A solvent-free complex of $\text{Cu}(\mathbf{2a})$ was obtained from toluene. The quality of the crystals was too low for a precise X-ray structure determination; however, the motif clearly shows isolated dinuclear units with higher symmetry as in the solvated complex.

In contrast to the derivatives of amino deoxysugars, the complexes $\text{Cu}(\mathbf{5a})$ and $\text{Cu}(\mathbf{5c})$, derived from aminocyclohexanol, contain solvent-free tetranuclear units with the “normal” cubane-like structure that is typical for complexes **I** with derivatives of simple 2-aminoethanol.^[10, 13–15] One monomer of $\text{Cu}(\mathbf{5c})$ (with the atom-numbering scheme), as well as the whole heterocubane structures of $[[\text{Cu}(\mathbf{5a})]_4]$ and $[[\text{Cu}(\mathbf{5c})]_4]$ are displayed in Figures 6 and 7, respectively. Selected bond

Figure 6. Atom-numbering scheme of the mononuclear formula unit of $\text{Cu}(\mathbf{5c})$ (with two coordinated oxygens of neighboring molecules); the same numbering scheme (without O4a, C13a) is used for $\text{Cu}(\mathbf{5a})$.

lengths and angles as well as nonbonding distances are listed in Table 5 and Table 6. A closer look reveals that both

Table 5. Selected interatomic distances, and bond lengths [Å] and bond angles [°] in $[[\text{Cu}(\mathbf{5a})]_4]$.

Cua–N1a	1.913(4)	Cua–O1a	1.920(3)
Cua–O2c	1.950(3)	Cua–O2a	1.986(3)
Cua–O2b	2.442(4)	Cub–O1b	1.921(3)
Cub–N1b	1.923(4)	Cub–O2d	1.947(3)
Cub–O2b	1.977(3)	Cub–O2a	2.442(3)
Cuc–O1c	1.921(3)	Cuc–N1c	1.912(3)
Cuc–O2b	1.948(3)	Cuc–O2c	1.984(3)
Cuc–O2d	2.539(3)	Cud–O1d	1.919(3)
Cud–N1d	1.911(4)	Cud–O2a	1.960(3)
Cud–O2d	1.975(3)	Cud–O2c	2.401(3)
Cua...Cub	3.387(3)	Cua...Cuc	3.102(3)
Cua...Cud	3.092(3)	Cub...Cuc	3.169(3)
Cub...Cud	3.113(3)	Cuc...Cud	3.438(3)
N1a–Cua–O1a	92.7(1)	N1a–Cua–O2c	170.2(1)
N1a–Cua–O2a	84.8(1)	N1a–Cua–O2b	109.5(1)
O1a–Cua–O2c	93.8(1)	O1a–Cua–O2a	173.5(1)
O1a–Cua–O2b	106.1(1)	O2c–Cua–O2a	88.0(1)
O2c–Cua–O2b	75.8(1)	O2a–Cua–O2b	80.4(1)
N1b–Cub–O1b	92.2(2)	N1b–Cub–O2d	169.5(1)
N1b–Cub–O2b	85.3(1)	N1b–Cub–O2a	110.7(1)
O1b–Cub–O2d	93.8(1)	O1b–Cub–O2b	175.0(1)
O1b–Cub–O2a	104.5(1)	O2d–Cub–O2b	88.1(1)
O2d–Cub–O2a	76.1(1)	O2b–Cub–O2a	80.5(1)
N1c–Cuc–O1c	92.3(1)	N1c–Cuc–O2b	167.7(1)
N1c–Cuc–O2c	85.1(1)	N1c–Cuc–O2d	114.3(1)
O1c–Cuc–O2b	93.8(1)	O1c–Cuc–O2c	173.2(1)
O1c–Cuc–O2d	109.4(1)	O2b–Cuc–O2c	87.7(1)
O2b–Cuc–O2d	73.6(1)	O2c–Cuc–O2d	77.4(1)
N1d–Cud–O1d	92.3(1)	N1d–Cud–O2a	168.5(1)
N1d–Cud–O2d	85.3(1)	N1d–Cud–O2c	111.2(1)
O1d–Cud–O2a	93.4(1)	O1d–Cud–O2d	174.0(1)
O1d–Cud–O2c	105.0(1)	O2a–Cud–O2d	88.1(1)
O2a–Cud–O2c	77.0(1)	O2d–Cud–O2c	81.0(1)

Table 6. Selected interatomic distances, and bond lengths [Å] and angles [°] in [[Cu(5c)]₄].

Cua–N1a	1.916(7)	Cua–O2a	1.913(6)
Cua–O2c	1.954(6)	Cua–O1a	1.967(5)
Cua–O2b	2.453(7)	Cub–O1b	1.911(6)
Cub–N1b	1.920(7)	Cub–O2d	1.962(5)
Cub–O2b	1.962(5)	Cub–O1a	2.414(6)
Cuc–O1c	1.903(7)	Cuc–N1c	1.907(7)
Cuc–O2b	1.959(5)	Cuc–O2c	1.970(6)
Cuc–O2d	2.441(7)	Cud–O1d	1.917(6)
Cud–N1d	1.904(7)	Cud–O1a	1.953(6)
Cud–O2d	1.973(5)	Cud–O2c	2.513(7)
Cua...Cub	3.342(5)	Cua...Cuc	3.123(5)
Cua...Cud	3.166(5)	Cub...Cuc	3.131(5)
Cub...Cud	3.114(5)	Cuc...Cud	3.415(5)
N1a–Cua–O2a	91.6(3)	N1a–Cua–O2c	170.0(3)
N1a–Cua–O1a	84.9(3)	N1a–Cua–O2b	109.7(3)
O2a–Cua–O2c	95.1(3)	O2a–Cua–O1a	173.1(3)
O2a–Cua–O2b	106.1(3)	O2c–Cua–O1a	87.7(2)
O2c–Cua–O2b	75.6(3)	O1a–Cua–O2b	80.7(3)
N1b–Cub–O1b	91.8(3)	N1b–Cub–O2d	167.6(2)
N1b–Cub–O2b	84.9(2)	N1b–Cub–O1a	112.9(3)
O1b–Cub–O2d	95.7(2)	O1b–Cub–O2b	176.6(2)
O1b–Cub–O1a	99.9(2)	O2d–Cub–O2b	87.5(2)
O2d–Cub–O1a	75.6(2)	O2b–Cub–O1a	81.8(2)
N1c–Cuc–O1c	92.0(3)	N1c–Cuc–O2b	167.3(3)
N1c–Cuc–O2c	85.7(3)	N1c–Cuc–O2d	114.5(3)
O1c–Cuc–O2b	93.1(2)	O1c–Cuc–O2c	174.3(3)
O1c–Cuc–O2d	104.8(3)	O2b–Cuc–O2c	88.1(2)
O2b–Cuc–O2d	75.3(3)	O2c–Cuc–O2d	81.0(3)
N1d–Cud–O1d	92.4(3)	N1d–Cud–O1a	168.0(3)
N1d–Cud–O2d	85.4(3)	N1d–Cud–O2c	113.8(3)
O1d–Cud–O1a	94.5(3)	O1d–Cud–O2d	175.9(3)
O1d–Cud–O2c	105.0(3)	O1a–Cud–O2d	87.1(2)
O1a–Cud–O2c	73.7(3)	O2d–Cud–O2c	79.1(3)

complexes form a β -type^[15] cubane structure, that is, the longer copper–oxygen bond pairs are arranged “perpendicularly”. Although the ligand molecule has two chiral centers, both complexes crystallize in nonchiral space groups. A closer look at the individual monomers of the tetranuclear complex reveals that the four ligands exist as two pairs of two enantiomers (pure *trans*-diastereomer, *R,R* and *S,S* configuration, of the aminoalcohol was used for syntheses).

Cu(5a) and Cu(5c) both consist of four mononuclear units, with the copper atoms coordinated to three donor atoms of their own tridentate ligand and two additional alcoholate oxygen atoms of neighboring molecules. One of these oxygen atoms occupies the axial position of the distorted square-pyramidal coordination sphere with a bond length of 240–254 pm. The Cu–Cu distances were found to be relatively similar (≈ 310 – 340 pm). As Figure 7b shows, the outer sphere of the complex molecule of Cu(5c) contains the cyclohexyl and ethyl carbon atoms. Therefore, no hydrogen bonding can be observed. This is a good explanation for the excellent solubility in nonpolar solvents, such as benzene, toluene, or chloroform. In Cu(5a), the noncoordinating acetyl oxygen atoms have long hydrogen-bonding contacts to the acetyl methyl groups of neighboring molecules with an average distance of O...H–C of 337 pm.

Altogether, a comparison of the structures discussed here clearly shows the strong effect of the sugar moiety on the structure and, therefore, on the chemistry of the oligonuclear complexes.

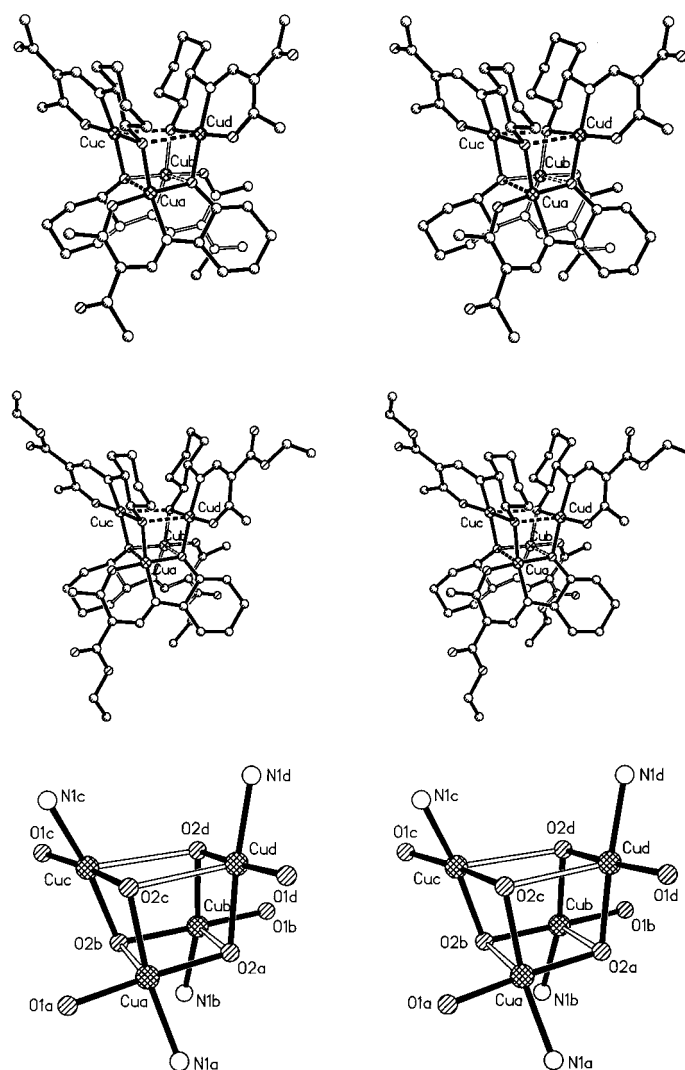


Figure 7. Stereoview of the tetranuclear molecular structures of a) [[Cu(5a)]₄] and b) [[Cu(5c)]₄]; c) the coordination mode of [[Cu(5c)]₄].

IR and UV/Vis spectra: The vibrational spectra of all complexes show that the absorptions of the chelated ligands are not significantly different from those of the free ligands. All electronic spectra show a d–d band in the region between $\lambda = 620$ and 675 nm with an extinction coefficient of about $150 \text{ dm}^3 \text{ mol}^{-1}$, and a ligand-to-metal charge-transfer absorption at $\lambda \approx 370$ nm. With respect to the dependence on concentration (varied over more than one order of magnitude), the spectra strongly follow the Lambert–Beer law, and there is no indication of the dissociation of the oligonuclear structures. Furthermore, EPR spectra of Cu(1a) in solution and in the solid state (see Figure 8) show the same signals; this indicates a similar structure.

Mass spectra: The mass spectrum of [[Cu(1a)]₂·Cu(OAc)₂] shows the mole peak of this trinuclear unit. This is also found in the MS of the new compound Cu(1b), the structure of which has not yet been determined by X-ray analysis. The spectrum also indicates that this structure is not very stable and that a dinuclear species is involved in the system. The *m/z*

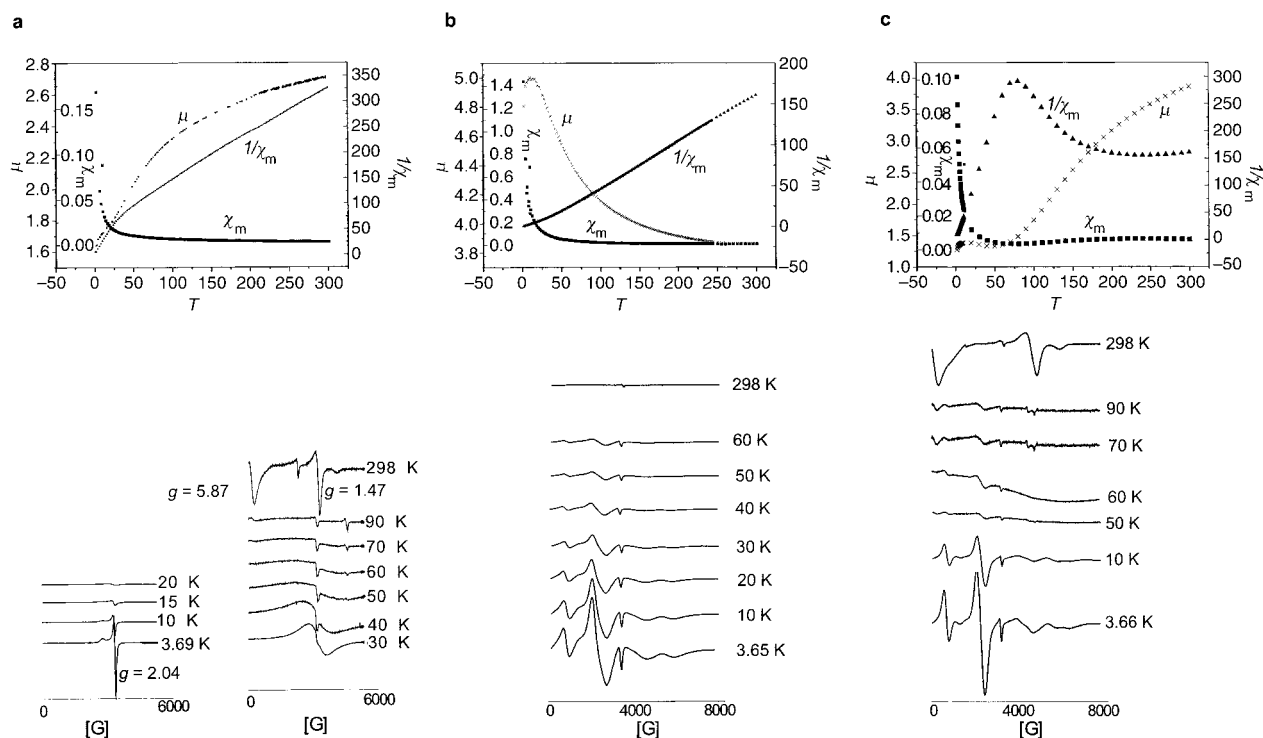
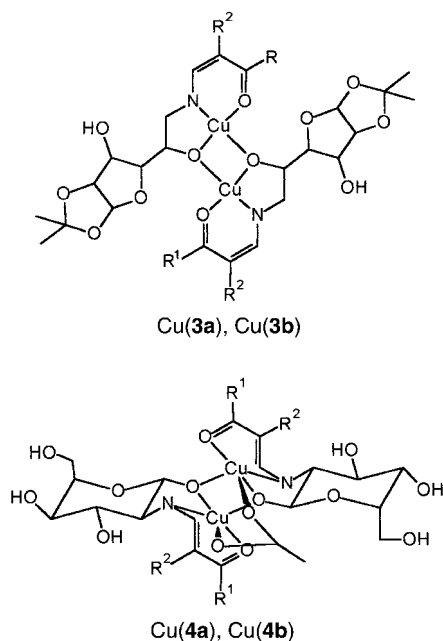


Figure 8. Magnetic behavior [χ_m vs T (\blacksquare); χ_m^{-1} vs T (\blacktriangle); magnetic moment vs T (\times); top], and EPR spectra (bottom) for a) $[\text{Cu}(\mathbf{1a})_2] \cdot \text{Cu}(\text{OAc})_2$ (EPR spectra: $\times 20$ for $T > 30$ K); b) $[\text{Cu}(\mathbf{5a})_4]_4$, and c) $[\text{Cu}(\mathbf{5c})_4]$.

peak of the dinuclear structure, determined by X-ray analysis, is also found for $\text{Cu}(\mathbf{2a})$ and for its analogue $\text{Cu}(\mathbf{2b})$. The ligands $\text{H}_2\mathbf{3}$ are isomers of the ligands of type $\text{H}_2\mathbf{2}$. The complexes $\text{Cu}(\mathbf{3a})$ and $\text{Cu}(\mathbf{3b})$, for which no suitable crystals for X-ray crystallography could be obtained, can therefore also be expected to form isomers of the complexes $\text{Cu}(\mathbf{2a})$ and $\text{Cu}(\mathbf{2b})$. Indeed, the mass spectra show the peaks of a dimer. This is a strong argument for the structure depicted in Scheme 3.



Scheme 3. Proposed structures for $\text{Cu}(\mathbf{3a})/\text{Cu}(\mathbf{3b})$ and $\text{Cu}(\mathbf{4a})/\text{Cu}(\mathbf{4b})$.

Similar to $\text{Cu}(\mathbf{3a})$ and $\text{Cu}(\mathbf{3b})$, the complexes derived from 2-amino-2-deoxyglucopyranose ligands $\text{H}_2\mathbf{4a,c}$, which have the composition $[\text{Cu}(\mathbf{4a})_2] \cdot (\text{Et}_3\text{NH})\text{OAc}$ and $[\text{Cu}(\mathbf{4c})_2] \cdot (\text{Et}_3\text{NH})\text{OAc}$, could not be crystallized in suitable quality for X-ray structure determination. The mass spectra of all of these compounds show the peaks of a $[\text{Cu}_2\text{L}_2(\text{OAc})]$ species. This is in agreement with the analytical data. The proposed structure is also depicted in Scheme 3. In addition, there are peaks of a species with the composition $[\text{Cu}_4\text{L}_4]$. This species should have a structure similar to that described for $\text{Cu}(\mathbf{5a})$ and $\text{Cu}(\mathbf{5c})$.

EPR spectra and magnetic measurements: The EPR spectra reflect the very different structures of the copper(II) complexes. The compounds $[\text{Cu}(\mathbf{4a})_2] \cdot (\text{Et}_3\text{NH})\text{OAc}$ and $[\text{Cu}(\mathbf{4c})_2] \cdot (\text{Et}_3\text{NH})\text{OAc}$ show the signals of isolated Cu^{II} atoms ($S = 1/2$), which are not coupled. The complexes $[\text{Cu}(\mathbf{2a})_2] \cdot \text{solv}$ are EPR-silent because of the strong antiferromagnetic coupling between the two copper centers within each dinuclear unit. This obeys a rule found for aminoethanol and aminopropanol β -ketoenaminic ligands of dicarbonyl compounds of type **I**:^[9–22] the compounds that form a saturated five-membered chelate ring with the alcoholate oxygen, and the nitrogen donor atoms show, in most cases, only weak or no antiferromagnetic coupling. Complexes with saturated six-membered chelate rings (or five-membered rings with sp^2 hybridization of the bridging atoms), however, show more or less strong antiferromagnetic coupling. The compounds $\text{Cu}(\mathbf{3a})$ and $\text{Cu}(\mathbf{3b})$ are further examples of compounds with five-membered rings; these spectra are similar to those of $[\text{Cu}(\mathbf{4a})_2] \cdot (\text{Et}_3\text{NH})\text{OAc}$ and $[\text{Cu}(\mathbf{4c})_2] \cdot$

(Et₃NH)OAc]. Of more interest are the spectra of the oligonuclear units [$\text{Cu}(\mathbf{1a})_2 \cdot \text{Cu}(\text{OAc})_2$] and [$\text{Cu}(\mathbf{1b})_2 \cdot \text{Cu}(\text{OAc})_2$]: in these spectra there are signals of a $S=1$ paramagnet (at $g=1.47$ and 5.87) and of a $S=1/2$ paramagnet (at $g=2.04$). The former disappear when the temperature is decreased, while latter ones become more intense (see Figure 8). This means that the copper atoms behave magnetically as two antiferromagnetically coupled Cu atoms and one isolated Cu atom. The spectra were fitted with the parameters given below to confirm this behavior.

Magnetic susceptibility was measured for the compounds between 300 K and 2 K. The results are in agreement with those obtained from EPR spectra. At room temperature, [$\text{Cu}(\mathbf{1a})_2 \cdot \text{Cu}(\text{OAc})_2$] has an effective magnetic moment of $2.71 \mu_B$. This is close to the spin-only value of an $S=1$ paramagnet. The temperature-dependent susceptibility measurement shows an antiferromagnetic coupling that leads to an effective moment of $1.64 \mu_B$ at 2 K, which is close to the spin-only value for an $S=1/2$ ground state. When the data are fitted with the results obtained from the EPR spectra, a value of $J=-309 \text{ cm}^{-1}$ is obtained; this value agrees with the strong coupling observed for aminopropanol derivatives.^[10–13] The complex of $\text{H}_2\mathbf{1b}$ behaves similarly; the data show only slight deviations.

Complexes [$\text{Cu}(\mathbf{2a})_2 \cdot \text{solv}$] and [$\text{Cu}(\mathbf{2b})_2 \cdot \text{solv}$] are diamagnetic over the whole temperature range from 300–2 K. This is remarkable because previously reported systems all show significant paramagnetism at room temperature. The coupling in our complexes represents one of the strongest observed for complexes with aminoalcohol Schiff-base ligands.

$\text{Cu}(\mathbf{3a})$ and $\text{Cu}(\mathbf{3b})$ show the paramagnetism of two magnetically nearly isolated copper atoms. The effective moment (calculated for the molecular mass of the dinuclear complex; expected value = $2.45 \mu_B$) is $2.14 \mu_B$ at room temperature and only slightly decreases to $1.47 \mu_B$ at 2 K because of weak antiferromagnetic coupling. The EPR spectra show the expected signals of a $S=1/2$ species at $g=2.06$. The intensity of which increases with decreasing temperature according to a Boltzmann-like behavior.

The 2-amino sugar derivatives, $\text{Cu}(\mathbf{4a})$ and $\text{Cu}(\mathbf{4c})$, have identical magnetic behavior and similar EPR spectra. They show very weak antiferromagnetic coupling with θ values of 5.4 and 2.3 K, respectively. Their EPR spectra show typical signals of $S=1/2$ paramagnets, as is to be expected from isolated copper(II) monomers. Indeed, there is typical Boltzmann-like increase in the signal intensity with decreasing temperature. The coupling-induced deviation from this behavior is very small and not significant.

Of great interest is the divergent magnetic behavior of $\text{Cu}(\mathbf{5a})$ and $\text{Cu}(\mathbf{5c})$ in spite of their very similar structures. Figure 8 shows the magnetic behavior and the EPR spectra of both compounds. Both show typical deviations from the Curie–Weiss law found for several of the cited compounds.^[10–22] Complex $\text{Cu}(\mathbf{5c})$ is a typical antiferromagnet, whereas $\text{Cu}(\mathbf{5a})$ shows weak ferromagnetic coupling.^[13] The magnetic behavior of cubane-type structures can be described by six coupling constants if the complex has only C_1 symmetry, as in $\text{Cu}(\mathbf{5a})$ and $\text{Cu}(\mathbf{5c})$. The similarity of all four copper centers in each of the two cubane structures makes it possible

to reduce the problem to two coupling constants (one for the longer and one for the shorter bridges). In this case, the magnetic behavior of such cubane-like clusters can be described by the Hamiltonian given in Equation (1):

$$H = -2J_{1,2}(S_1S_2 + S_3S_4) - 2J_{1,3}(S_1S_3 + S_1S_4 + S_2S_3 + S_2S_4)^{[36]} \quad (1)$$

which leads to Equation (2):

$$\chi = (1-x)[N_A\beta^2g^2/(4k(T-\theta))]\{(10e^{2u} + 2e^{-2u} + 4e^{-2v})/(5e^{2u} + 3e^{-2u} + 6e^{-2v} + e^{-4v})\} + x\chi_{\text{para}} \quad (2)$$

with $u = J_{1,3}/kT$; $v = J_{1,2}/kT$ and x = molar fraction of a paramagnetic impurity.

For $\text{Cu}(\mathbf{5c})$, the best fit was reached with the parameters $J_{1,3} = -4.7(2) \text{ cm}^{-1}$, $J_{1,2} = 7.6(3) \text{ cm}^{-1}$, $g = 2.34$ (fixed), and $\theta = 1.41 \text{ K}$; and for $\text{Cu}(\mathbf{5a})$ with the parameters $J_{1,3} = -25(2) \text{ cm}^{-1}$, $J_{1,2} = -13(2) \text{ cm}^{-1}$, $g = 1.95$ (fixed), and $\theta = -0.82 \text{ K}$.

The EPR spectra of $\text{Cu}(\mathbf{5a})$ show the expected increase in the intensity of the complex signal with decreasing temperature. The spectrum can be identified as that of an $S=2$ paramagnet with an additional $S=1/2$ signal. Indeed, the magnetic moment measured at 4 K of $4.94 \mu_B$ corresponds to the spin-only value of a $S=2$ paramagnet. The spectrum of $\text{Cu}(\mathbf{5c})$ undergoes a significant change from room temperature (298 K) to 3.66 K. The spectrum at liquid-helium temperature is very similar to that of $\text{Cu}(\mathbf{5a})$, whereas the spectrum at 298 K shows different signals which become weaker at lower temperature.

The magnetic moment of $\text{Cu}(\mathbf{5a})$ at room temperature of $3.86 \mu_B$ is significantly lower than that of an $S=2$ paramagnet and indicates that there are different mixtures between the possible spin states at every temperature. The remaining magnetic moment of $1.22 \mu_B$ shows that the antiferromagnetic ground state is not the only one populated at 4 K. The simulation of the EPR spectrum indicates that it can be interpreted as the one of four species with $S=1/2$, 1, $3/2$, and 2. (Parameters: $S=1/2$, $g_x = 2.058$, $g_y = 2.060$, $g_z = 2.264$, $A = 488 \text{ MHz}$; $S=1$, $D = 17710$, $E = 400$, $g_x = 2.8$, $g_y = 2.8$, $g_z = 2.965$; $S=3/2$, $D = 1$, $E = 0.33$, $g_x = g_y = g_z = 4.28$; $S=2$, $D = 17710$, $E = 400$, $g_x = 2.8$, $g_y = 2.8$, $g_z = 2.965$).

The existence of signals with $S=3/2$ and $S=1/2$ can be explained by the asymmetry of the structure: one of the longer Cu–O bonds in the cubane is 11 pm longer than the average value of the other three bonds. It is possible that coupling of this copper atom (Cuc) is much weaker than the others and results in a single copper signal with $S=1/2$ and a signal of the remaining three copper atoms with $S=3/2$.

The magnetic behavior of $\text{Cu}(\mathbf{5c})$ should therefore better be explained by the addition of a term for a “trinuclear” ($S=3/2$) species. The Hamiltonian for this is given in Equation (3):

$$H = -J(S_1S_2 + S_2S_3) - J'(S_1S_3)^{[36]} \quad (3)$$

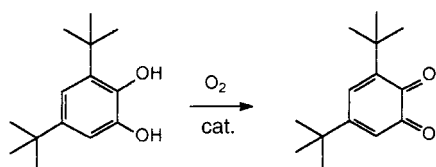
and leads to the second term for the susceptibility given in Equation (4):

$$\chi = x_1[N_A\beta^2g^2/(4k(T-\theta))]\{(10e^{2u} + 2e^{-2u} + 4e^{-2v})/(5e^{2u} + 3e^{-2u} + 6e^{-2v} + e^{-4v})\} + [N\beta^2/4kT]\{(g_x^2 + g_y^2)e^{(J-J'/kT)} + g_z^2e^{3J/2kT}\}/(1 + e^{(J-J)/kT} + 2e^{3J/2kT})\}x_2 + x_3\chi_{\text{para}} \quad (4)$$

where $u = J_{1,3}/kT$; $v = J_{1,2}/kT$; $g_1 = (4g_A - g_B)/3$; $g_2 = (2g_A + g_B)/3$; $g_3 = g_B$; x_1 = molar fraction of the $S=1$ and $S=2$ species; x_2 = molar fraction of the $S=1/2$ and $S=3/2$ species; and $x_3 = x_2$ + molar fraction of a paramagnetic impurity.

The best fit was attained for the following parameters: $g = 2.852$; $g_A = 2.127$; $g_B = 4.28$ (all g values were taken from the EPR spectrum); $x_1 = 0.9525$; $x_2 = 0.0475$; $x_3 = 0.0482$; $J_{1,3} = 25.4(2) \text{ cm}^{-1}$; $J_{1,2} = -21.4(2) \text{ cm}^{-1}$; $J = 0 \text{ cm}^{-1}$; $J' = -9.6(2) \text{ cm}^{-1}$.

Studies on catechol-oxidase-like activity: Prior to a detailed kinetic study, an overview of the catalytic ability of the complexes is necessary. To evaluate qualitatively a significant activity, 10^{-4} M solutions of the complexes were treated with 50 equivalents of di-*tert*-butylcatechol (dtbc).



The observed reactivities were compared with that of copper(II) acetate under the same conditions. Only the complexes that show a significantly higher activity than copper acetate were considered to be active and kinetic measurements were carried out. The activities of the complexes are very different: while Cu(3a) is highly active, some complexes have low or no catalytic activity. Stoichiometric amounts of dtbc were added to the catalyst solutions, and this was repeated until the absorption reached the limit at which a linear correlation between concentration and absorption is no longer valid. For every addition, the initial rate stayed at the same value, and no change of the spectra, except for the *o*-quinone band at $\lambda = 400 \text{ nm}$ ($\epsilon = 1900 \text{ M}^{-1} \text{ cm}^{-1}$), was observed so that the catalysts appear to be stable.

In accord with previous work by Reim and Krebs,^[5] spectrophotometric titrations of the complex solutions with tetrachlorocatechol (tcc) were carried out in order to obtain information about the binding of dtbc in the complexes. In comparison with dtbc, tcc has, owing to its electron-withdrawing substituents, a higher redox potential and is not oxidized to the corresponding quinone. Figure 9a shows the titration of one of the active complexes, Cu(4a), all of them show principally the same behavior, and one of the inactive complexes, Cu(4c). The spectrum of the active compound changes to a markedly higher degree than that of the inactive complex. In the charge-transfer region of $\lambda \approx 350\text{--}450 \text{ nm}$, the intensity decreases along with the d–d band of the complex at $\lambda \approx 650 \text{ nm}$. The more this band decreases, the higher is the activity found for the complexes. In addition, a new band at $\lambda \approx 480 \text{ nm}$ appears, which can be interpreted as a d–d band of a complex with a higher ligand field strength, for example, with coordinated catecholate, or as a CT band.^[52]

The kinetic data of the oxidation of dtbc were determined by the method of initial rates by monitoring the growth of the $\lambda = 400 \text{ nm}$ band of the resulting *o*-quinone. The dc/dt versus c_{cat} plots are shown in Figure 10a. A linear relationship between the initial rates and the complex concentration is

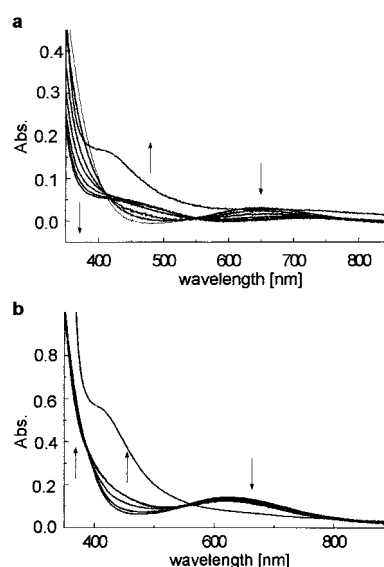


Figure 9. Spectrophotometric titration of a) an active complex Cu(4a) and b) an inactive Cu(4c) complex with 0.5–50 equivalents of tcc.

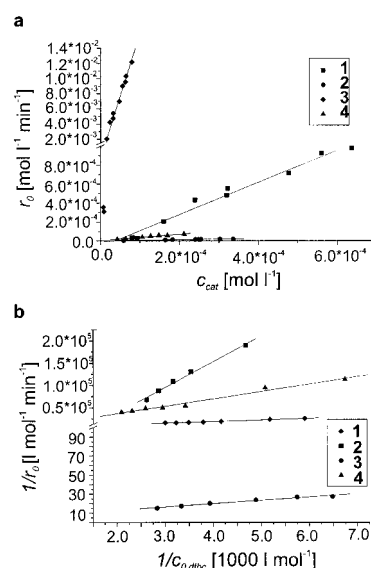
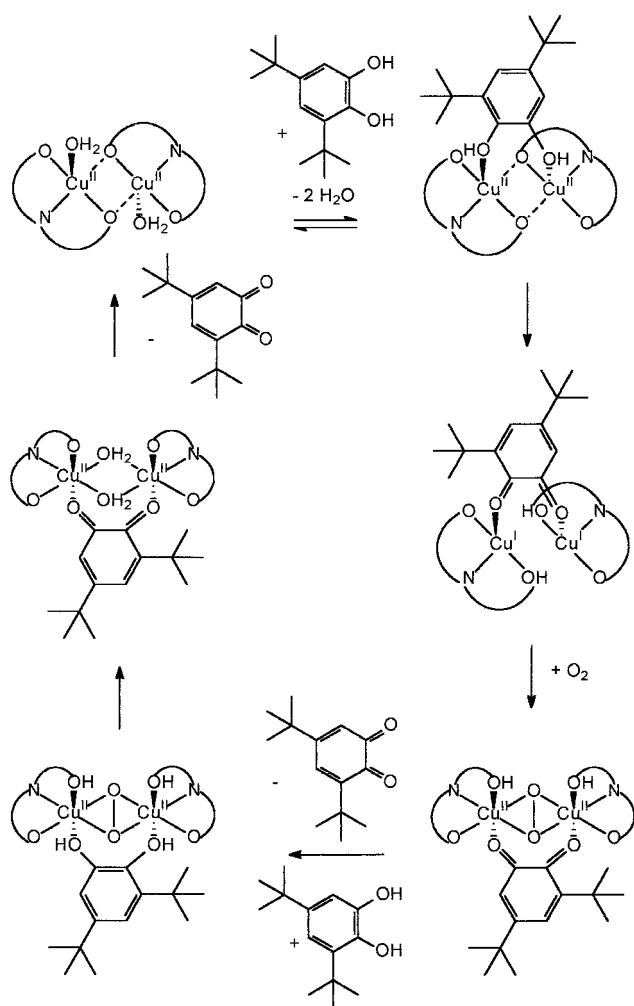


Figure 10. Catalytic activity of Cu(1a)–Cu(4a): a) rate dependence on catalyst concentration; b) Lineweaver–Burk plots.

obtained for all active compounds [Cu(1a)–Cu(4a)], which indicates a first-order dependence of the rate on the catalyst concentration. When the complexes were treated with varying amounts of dtbc, a first-order dependence on the substrate concentration was observed at low concentrations. At higher concentrations, all four compounds showed saturation kinetics. A treatment on the basis of the Michaelis–Menten model was therefore appropriate. The Lineweaver–Burk plots are given in Figure 10b. We propose a pre-equilibrium between the free complex and the substrate. The subsequent redox processes and the substitution of one quinone by a second catechol are irreversible (rate-determining) steps. Although the real mechanism of the reaction might be more complicated (see Scheme 4), the data taken from this simple model are sufficient for a comparison of the catalytic activity (Table 7).



Scheme 4. Possible mechanism of dtbc oxidation catalyzed by dinuclear copper complexes (adapted from refs. [47, 48]).

Table 7. Kinetic data of dtbc oxidation catalyzed by selected copper(II) complexes.

Cu catalyst from	c_{cat} [molL ⁻¹]	k_{cat} [h ⁻¹]	K_{M} [molL ⁻¹]	k [h ⁻¹]
H ₂ 1a	1.45×10^{-4}	$138 \pm 8^{\text{[a]}}$	$(8.94 \pm 0.5) \times 10^{-4^{\text{[a]}}}$	$102 \pm 4^{\text{[b]}}$
H ₂ 2a	4.5×10^{-4}	2.8 ± 0.3	$(7.08 \pm 0.5) \times 10^{-4}$	4.0 ± 0.2
H ₂ 3a	5.47×10^{-5}	9471 ± 255	$(5.90 \pm 0.4) \times 10^{-3}$	9927 ± 392
H ₂ 4a	2.07×10^{-4}	61.5 ± 1.7	$(5.45 \pm 0.5) \times 10^{-3}$	60.2 ± 1.0

[a] Standard deviation obtained from three measurements (correlation coefficient r of the Lineweaver–Burk plot ≥ 0.992). [b] Standard deviation obtained from three measurements (correlation coefficient r of the r_0 vs c_{cat} plot ≥ 0.99).

As the obtained data show, Cu(3a), Cu(1a), and Cu(4a) are effective catalysts for the oxidation of dtbc to dtbq. The complex Cu(2a) shows only little activity, although its structure is similar to the proposed structures of Cu(3a) and Cu(4a). The k values obtained from the variation of the catalyst concentrations are also given in Table 7 and are similar to the k_{cat} values obtained from the Michaelis–Menten model. The explanation of the divergent behavior of Cu(3a) and Cu(4a) relative to Cu(2a) is the existence of a five-membered chelate ring in the first-named compounds, whereas Cu(2a) contains only six-membered chelate rings. Thus, Cu(3a) and Cu(4a) should deviate more from square-planar geometry than Cu(2a). Former investigations^[3–7, 37–46]

showed that a square-planar geometry is not ideal for a possible catechol-oxidase catalyst.

Karlin^[47] and Casella^[48] suggested a mechanism for the oxidation of catechols to *o*-quinones by dinuclear copper complexes. Although no strong evidence exists, some of our observations indicate a mechanism which is analogous to that previous described. This mechanism—adapted for our compounds—is shown in Scheme 4.

In the first step, two solvent molecules (e.g., water) are substituted by a catechol molecule. Two protons are then transferred to the bridging alkoxide groups. Simultaneously, two electrons of the catecholate reduce the copper(II) to form a dinuclear copper(I) species with the *o*-quinone as a ligand. A dioxygen molecule enters to reoxidize both copper(I) and to form a μ -peroxo species with copper(II). The *o*-quinone, which is a weaker σ -donor and a stronger π -acceptor ligand than catecholate and which is therefore bound more weakly to copper(II) than to copper(I), is replaced by a second catechol molecule. This should be the slowest step. Two protons and two electrons of this catechol as well as two protons of the bridging chelate ligands are transferred to the peroxo bridge. The last step is the loss of a second quinone molecule and the reformation of the original catalyst.

No observations were made that contradict such a mechanism; however, some arguments support this interpretation: the electronic spectra of the complexes obey the Lambert–Beer law and the solid-state and solution (toluene) EPR spectra of Cu(1a) are identical. This means that there is no indication of a dissociation of the oligonuclear species in solution. Furthermore, the solutions contain several possible bridging ligands, for example, water, methanol, acetate, and, as the titration with tetrachlorocatechol showed, the catechol substrate itself might react as a (probably dianionic) bridging ligand. Therefore, the catalysts should react as oligonuclear species. If the substrate is added to the catalysts under an inert atmosphere (Ar), a stoichiometric reaction takes place. For a compound with a similar structure based on an aminoalcohol derivative of a steroid,^[49] a species with the composition [Cu₂L₂(dtbc)] was isolated and characterized by ¹H NMR and mass spectroscopy.

The addition of hydrogen peroxide to Cu(4a) leads to bands at $\lambda = 350$ and 550 nm, which are typical for the μ - η^2 : η^2 -peroxo species.^[50–52] This species is also well-known for type III copper enzymes, such as catechol oxidase.^[1–3] Therefore, it can be assumed that the dioxygen reacts with the dicopper(I) species to give the named peroxo species.

Although Cu(1a) also has only six-membered chelate rings, it is, unlike Cu(2a), an effective catalyst. The difference, compared to Cu(2a), is that the copper coordination geometry is much more distorted and, on account of its trinuclear structure, it may react in a different way. This example reveals one feature of the interesting potential of carbohydrate derivatives as complex ligands: the unusual oligomerization in Cu(1a) is caused by the carbohydrate's additional donor functions and leads to an active catalyst. For compounds with five-membered chelate rings between the alcoholate oxygen and the enamine nitrogen atom, a cubane structure should be expected, as in Cu(5a), Cu(5c), and several other examples.^[10–22] Nevertheless, the aminocarbohydrate com-

pounds of type Cu(**3a**) and Cu(**4a**) show dimeric species which have, in contrast to the cubanes, copper centers that are accessible to substrates.

The importance of the substituents R¹ and R² is shown by the inactivity of Cu(**1b**)–Cu(**3b**) and Cu(**4c**). Only the combination R¹ = CH₃, R² = COCH₃ leads to active catalysts. The strong effect of these peripheral substituents is evident, even for the heterocubane compounds of type Cu(**5**): the change in R² from an ethylcarboxylate group [Cu(**5c**)] to an acetyl group [Cu(**5a**)] changes the magnetic behavior from antiferromagnetic to ferromagnetic coupling.

Experimental Section

Chemicals: The solvents for synthesis of the complexes Cu(**4a**) and Cu(**4c**) and for measurements were distilled under an argon atmosphere prior to use. Methanol was dried by reaction with magnesium. Chemicals were obtained from Fluka and Aldrich.

Spectroscopic measurements: Electronic spectra were measured with a Varian Cary1 or Cary5E spectrophotometer at room temperature. EPR spectra were, if possible (only for Cu(**1a**), Cu(**5a**), and Cu(**5c**)), obtained in frozen toluene solutions at 77 K and in solution at room temperature; for the solids (all compounds) they were obtained at these temperatures as well as at temperatures down to 3.8 K with liquid helium. Measurements took place in the X band at 9.75 GHz on a BRUKER ERS300 spectrometer equipped with a flowing-nitrogen variable-temperature controller.

IR spectra were measured on a Perkin–Elmer 2000 spectrometer, NMR spectra on a Bruker AC-200, and mass spectra were carried out on a Finnigan MATSSQ 710 or a Finnigan MAT95XLTRAP. Elemental analyses were carried out on a Leco CHNS 932.

Procedures for the kinetic measurements: All kinetic measurements were carried out in methanol because of the good solubility of the substances used. For detection of the reaction, the intense absorption of the resulting quinone ($\lambda = 400$ nm, $\epsilon = 1900$ mol⁻¹ dm³ cm⁻¹) was used. Blind measurements were carried out without the presence of a possible catalyst and in the presence of the copper acetate monohydrate used for complex synthesis. The copper acetate measurement was used to decide if a complex showed activity or not. For this, a 10⁻⁴ M solution of the complex was made and 50 equiv of di-*tert*-butylcatechol (dtbc) was added. The spectra were recorded every 2 min. In a repeated experiment, the slope of the absorption at $\lambda = 400$ nm against time was recorded. The initial rate obtained from this slope was compared to the rate with copper acetate. Further investigations were only carried out with those complexes that had higher rates. Initially, the above-named amount of dtbc was added to different concentrations of the catalysts between 5 × 10⁻⁵ and 1 × 10⁻³ M for Cu(**1a**), Cu(**2a**), and Cu(**4a**) and between 5 × 10⁻⁶ and 1 × 10⁻⁴ M for Cu(**3a**) in order to determine the kinetic behavior towards the variation of the catalyst concentration. To determine the rate constants for the variation of the substrate concentration, the amount of dtbc was varied to find the region of concentration at which saturation is observed. The initial rates of the reaction were obtained and compiled to give a Lineweaver–Burk plot. To reduce the statistical error, every measurement was carried out at least three times, only those measurements were taken into account in which the discrepancy value of the linear fit was at least 0.992.

To understand the binding of dtbc in the complexes, spectrophotometric titrations of the complexes with the substrate analogue tetrachlorocatechol (tcc) were carried out with 2 × 10⁻⁴ M solutions of the catalysts and 0.01 M solutions of tcc. The spectra were recorded for steps of 0.5 equivalents (addition of 20 μ L to 2 mL solution) up to the saturation point.

General synthesis of ligands H₂1a,b–H₂3a,b and their copper complexes: The aminocarbohydrate compounds were obtained via their azides, which were synthesized according to literature.^[35a–g] The azides were reduced with Raney-Nickel (see, for example, ref. [35h, i]).

The amino sugar (0.5 mmol) was dissolved in methanol (15 mL). Triethylamine (202 mg, 2 mmol) and 3-ethoxymethylen-2,4-pentandione (0.5 mmol; H₂1a–H₂3a) or 2-ethoxymethylene malonic acid diethyl ester

(0.5 mmol; H₂1b–H₂3b) were added dropwise. After stirring for 1–12 h, when the formation of the ligand was complete (TLC), copper acetate monohydrate (136 mg, 0.75 mmol for Cu(**1a**) and Cu(**1b**) or 91 mg, 0.5 mmol for Cu(**2a**), Cu(**2b**), Cu(**3a**), and Cu(**3b**)) was added. The mixture was left to stand overnight and the solvent was evaporated to leave the rare product.

Spectroscopic data of the ligands H₂1a,b–H₂3a,b:

H₂1a: ¹H NMR (200 MHz, CDCl₃, 25 °C, TMS): $\delta = 4.81$ (d, 1 H; H1), 3.20 (dd, 1 H; H2), 3.35–3.70 (m, 4 H; H3, H4, H5, H6), 3.32 (dd, 1 H; H6'), 11.02 (dd, 1 H; N–H), 7.74 (d, 1 H; =CH–), 2.22 (s, 3 H; CH₃), 2.44 (s, 3 H; CH₃), 3.37, 3.46, 3.59 (m, 9 H; 3 × OCH₃), 2.89 (1 H; OH); ¹³C NMR (200 MHz, CDCl₃, 25 °C, TMS): $\delta = 97.59$ (C1), 82.50 (C2), 70.73 (C3), 81.81 (C4), 69.66 (C5), 61.24 (C6), 200.39, 194.49 (C=O), 111.68 (=C–), 160.87 (=CH–), 27.21, 31.83 (CH₃), 50.57, 55.42, 58.43 (OCH₃); MS (DCI with H₂O): m/z : 332 [M+H]⁺; elemental analysis calcd (%) for C₁₅H₂₅NO₇ (331.36): C 54.37, H 7.60, N 4.23; found C 53.94, H 7.74, N 3.94.

H₂1b: ¹H NMR (200 MHz, CDCl₃, 25 °C, TMS): $\delta = 4.80$ (d, 1 H; H1), 3.19 (dd, 1 H; H2), 3.35–3.70 (m, 4 H; H3, H4, H5, H6), 3.29 (dd, 1 H; H6'), 9.27 (dd, 1 H; N–H), 7.98 (d, 1 H; =CH–), 1.21–1.32 (m, 6 H; 2 × CH₃), 3.35, 3.45, 3.59 (m, 9 H; 3 × OCH₃), 4.10–4.24 (m, 4 H; 2 × CH₂), 2.82 (1 H; OH); ¹³C NMR (200 MHz, CDCl₃, 25 °C, TMS): $\delta = 97.45$ (C1), 82.61 (C2), 70.58 (C3), 81.79 (C4), 69.84 (C5), 60.34 (C6), 169.14, 166.21 (C=O), 90.05 (=C–), 160.71 (=CH–), 14.30, 14.40 (CH₃), 59.60, 59.75 (CH₂) 50.15, 55.28, 58.41 (OCH₃); MS (DCI with H₂O): m/z : 392 [M+H]⁺; elemental analysis calcd (%) for C₁₇H₂₉NO₉ (391.42): C 52.17, H 7.47, N 3.58; found C 52.43, H 7.59, N 3.56.

H₂2a: M.p. 152 °C; ¹H NMR (200 MHz, CDCl₃, 25 °C, TMS): $\delta = 5.87$ (d, 1 H; H1), 4.49 (d, 1 H; H2), 4.30 (s, 1 H; H3), 3.90 (d, 1 H; H4), 4.04 (m, 1 H; H5), 3.65 (m, 1 H; H6), 3.43 (m, 1 H; H6'), 10.97 (m, 1 H; N–H), 7.81 (d, 1 H; =CH–), 1.25, 1.38 (m, 6 H; 2 × CH₃), 2.21, 2.37 (m, 6 H; 2 × CH₃); ¹³C NMR (200 MHz, CDCl₃, 25 °C, TMS): $\delta = 104.97$ (C1), 85.18 (C2), 74.20 (C3), 80.34 (C4), 67.84 (C5), 53.51 (C6), 200.68, 195.71 (C=O), 111.87 (=C–), 161.73 (=CH–), 27.10, 31.83 (CH₃), 26.63, 26.11 (CMe₂), 111.37 (CMe₂); MS (DCI with H₂O): m/z : 330 [M+H]⁺; elemental analysis calcd (%) for C₁₅H₂₃NO₇ (329.34): C 54.70, H 7.04, N 4.25; found C 54.59, H 7.09, N 4.22.

H₂2b: M.p. 55 °C; ¹H NMR (200 MHz, CDCl₃, 25 °C, TMS): $\delta = 5.88$ (d, 1 H; H1), 4.48 (d, 1 H; H2), 4.33 (s, 1 H; H3), 3.85–4.30 (m, 6 H; H4, H5, 2 × CH₂), 3.60 (m, 1 H; H6), 3.39 (m, 1 H; H6'), 9.26 (m, 1 H; N–H), 7.98 (d, 1 H; =CH–), 1.20–1.50 (m, 12 H, 4 × CH₃); ¹³C NMR (200 MHz, CDCl₃, 25 °C, TMS): $\delta = 105.07$ (C1), 85.12 (C2), 74.43 (C3), 80.72 (C4), 68.39 (C5), 53.08 (C6), 171.25, 168.81 (C=O), 89.35 (=C–), 160.69 (=CH–), 14.27, 14.09 (CH₃), 59.92, 59.88 (CH₂), 26.72, 26.16 (CMe₂), 111.82 (CMe₂); MS (DCI with H₂O): m/z : 390 [M+H]⁺; elemental analysis calcd (%) for C₁₇H₂₇NO₉ (389.40): C 52.44, H 6.99, N 3.60; found C 52.02, H 7.22, N 3.06.

H₂3a: M.p. 177 °C; ¹H NMR (200 MHz, CDCl₃, 25 °C, TMS): $\delta = 5.84$ (d, 1 H; H1), 4.42 (d, 1 H; H2), 3.97 (s, 1 H; H3), 4.15 (d, 1 H; H4), 3.77 (m, 1 H; H5), 3.62 (m, 1 H; H6), 3.62 (m, 1 H; H6'), 10.87 (dd, 1 H; N–H), 7.97 (d, 1 H; =CH–), 1.22, 1.38 (m, 6 H; 2 × CH₃), 2.15, 2.28 (m, 6 H; 2 × CH₃), 5.11 (m, 1 H; O–H6), 5.70 (d, 1 H, O–H3); ¹³C NMR (200 MHz, CDCl₃, 25 °C, TMS): $\delta = 104.35$ (C1), 84.86 (C2), 73.19 (C3), 84.86 (C4), 60.30 (C5), 60.50 (C6), 197.81, 193.86 (C=O), 110.70 (=C–), 161.00 (=CH–), 27.09, 31.49 (CH₃), 26.62, 26.07 (CMe₂), 110.38 (CMe₂); MS (DCI with H₂O): m/z : 330 [M+H]⁺; elemental analysis calcd (%) for C₁₅H₂₃NO₇ (329.35): C 54.70, H 7.04, N 4.25; found C 54.72, H 7.30, N 4.29.

H₂3b: M.p. 157 °C; ¹H NMR (200 MHz, CDCl₃, 25 °C, TMS): $\delta = 5.90$ (d, 1 H; H1), 4.49 (d, 1 H; H2), 4.07–4.22 (m, 6 H; H3, H4, 2 × CH₂), 3.70–3.95 (m, 3 H; H5, H6, H6'), 9.35 (dd, 1 H; N–H), 8.03 (d, 1 H; =CH–), 1.20–1.45 (m, 12 H, 4 × CH₃); ¹³C NMR (200 MHz, CDCl₃, 25 °C, TMS): $\delta = 104.85$ (C1), 85.30 (C2), 74.33 (C3), 78.77 (C4), 62.47 (C5), 62.47 (C6), 168.98, 166.96 (C=O), 90.14 (=C–), 160.09 (=CH–), 14.30 (CH₃), 59.89 (CH₂), 26.72, 26.10 (CMe₂), 111.92 (CMe₂); MS (DCI with H₂O): m/z : 390 [M+H]⁺; elemental analysis calcd (%) for C₁₇H₂₇NO₉ (389.40): C 52.44, H 6.99, N 3.60; found C 52.44, H 7.11, N 3.60.

Bis[1,2,3-O-trimethyl-6-N-(3-acetylbut-3-en-2-one)amino-6-deoxyglucopyranosyl]bis- μ -acetatocopper(II), Cu(1a**):** Isolation of Cu(**1a**): The residue was dissolved in diethyl ether. Blue crystals of Cu(**1a**) precipitated during the slow evaporation of the solvent. Yield: 187 mg (38.7%); IR (KBr): $\tilde{\nu} = 3321$ (vw), 2980 (s), 2915 (s), 2845 (s), 1721 (vw), 1647 (w), 1626 (w), 1592 (vs), 1545 (vs), 1475 (w), 1395 (vs), 1352 (s), 1282 (s), 1196 (w), 1147 (s), 1081 (vs), 1047 (vs), 1022 (s), 995 (s), 955 (s), 937 (s), 745 (s), 647 (vs),

615 cm⁻¹ (vs); UV/Vis (MeOH): λ (ϵ) = 659 (319), 357 nm (2530 mol⁻¹ dm³ cm⁻¹); MS (DEI): m/z : 967 [M]⁺, 908 [M - OAc]⁺, 849 [M - 2 × OAc]⁺, 785 [Cu₂L₂]⁺, 515 [Cu₂L(OAc)]⁺, 452 [CuL(OAc)]⁺, 393 [CuL]⁺; elemental analysis calcd (%) for C₃₄H₅₄N₂O₁₈Cu₃ (967.42): C 42.21, H 5.42, N 2.90, Cu 19.7; found C 41.79, H 5.54, N 2.87, Cu 19.5.

Bis[1,2,3-*O*-trimethyl-6-*N*-(2,2-bisethylcarboxyethylene)amino-6-deoxyglucopyranosyl]bis- μ -acetatotricopper(II), Cu(1b): Cu(1b) was isolated in a similar manner to Cu(1a). Yield: 174 mg (33.9%); IR (KBr): $\tilde{\nu}$ = 3436 (w), 3279 (w), 2980 (s), 2934 (s), 2907 (s), 2836 (w), 1702 (s), 1684 (s), 1657 (s), 1613 (vs), 1553 (s), 1499 (w), 1553 (s), 1430 (s), 1399 (w), 1379 (w), 1346 (w), 1272 (w), 1244 (s), 1218 (s), 1156 (w), 1139 (w), 1061 (vs), 1047 (vs), 1024 (vs), 959 (s), 918 (w), 802 (s), 791 (s), 734 (s), 621 cm⁻¹ (w); UV/Vis (toluene): λ (ϵ) = 664 (435), 397 (1469), 346 nm (1773 mol⁻¹ dm³ cm⁻¹); MS (FAB): m/z : 1028 [Cu₂L₂(OAc)]⁺, 969 [Cu₂L₂]⁺, 905 [Cu₂L₂]⁺, 453 [CuL]⁺, 392 [H₂L+H]⁺; elemental analysis calcd (%) for C₃₈H₆₀N₂O₂₂Cu₃ (1087.53): C 42.08, H 5.49, N 2.73, Cu 18.6; found C 42.39, H 5.39, N 2.77, Cu 18.5.

Bis[1,2-*O*-isopropylidene-5-*N*-(3-acetylbut-3-en-2-one)amino-5-deoxyglucufuranosyl]dicopper(II)-bis[1,2-*O*-isopropylidene-5-*N*-(3-acetylbut-3-en-2-one)amino-5-deoxyglucufuranosyl]-methanolodicycopper(II) · 3H₂O, Cu(2a): Isolation of Cu(2a): The residue was dissolved in toluene. A violet toluene-containing compound crystallized during the slow evaporation of the solvent. Recrystallization from water/methanol = 1:1 led to the precipitation of Cu(2a) in a quality suitable for X-ray crystal-structure determination. Yield: 50 mg (24.00%); IR (KBr): $\tilde{\nu}$ = 3331 (w), 2984 (s), 2928 (s), 1719 (vw), 1649 (w), 1584 (vs), 1457 (s), 1395 (vs), 1357 (s), 1283 (s), 1257 (s), 1213 (s), 1165 (s), 1125 (s), 1059 (vs), 1008 (vs), 946 (s), 882 (s), 844 (s), 732 (s), 696 (w), 638 cm⁻¹ (s); UV/Vis (MeOH): λ (ϵ) = 651 (166), 373 nm (1344 mol⁻¹ dm³ cm⁻¹); MS (ESI): m/z : 1585 [Cu₄L₄+Na]⁺, 1173 [Cu₃L₃+H]⁺, 804 [Cu₂L₂+Na]⁺, 783 [Cu₂L₂H₂]⁺, 423 [CuL(MeOH)]⁺, 391 [CuL]⁺; elemental analysis calcd (%) for C₆₁H₉₆N₄O₃₃Cu₄ (1667.62): C 43.94, H 5.80, N 3.36, Cu 15.2; found C 44.05, H 5.87, N 3.31, Cu 15.1.

Bis[1,2-*O*-isopropylidene-5-*N*-(2,2-bisethylcarboxyethylene)amino-5-deoxyglucufuranosyl]dicopper(II), Cu(2b): The residue was extracted with toluene to give a blue solid. Yield: 110 mg (49%); IR (KBr): $\tilde{\nu}$ = 3426 (vw), 2955 (s), 2923 (vs), 2854 (vs), 1733 (vw), 1675 (w), 1604 (s), 1461 (s), 1412 (w), 1377 (s), 1347 (w), 1259 (s), 1215 (w), 1166 (w), 1068 (vs), 1013 (vs), 868 (w), 796 (vs), 727 (w), 642 cm⁻¹ (w); UV/Vis (toluene): λ (ϵ) = 583 (466), 352 nm (2794 mol⁻¹ dm³ cm⁻¹); MS (ESI): m/z : 2728 [Cu₄L₄+Na]⁺, 1827 [Cu₄L₄+Na]⁺, 1353 [Cu₃L₃]⁺, 925 [Cu₂L₂+Na]⁺; elemental analysis calcd (%) for C₃₄H₅₀N₂O₁₈Cu₂ (C 45.28, H 5.59, N 3.11, Cu 14.1; found C 45.47, H 5.48, N 3.21, Cu 14.1.

Bis[1,2-*O*-isopropylidene-6-*N*-(3-acetylbut-3-en-2-one)amino-6-deoxyglucufuranosyl]dicopper(II), Cu(3a): Cu(3a) was isolated by recrystallization of the residue from a mixture of toluene, chloroform, and ethanol (2:2:1). Yield: 122 mg (62%); IR (KBr): $\tilde{\nu}$ = 3314 (w), 2961 (s), 2925 (vs), 2854 (s), 2683 (vw), 1724 (w), 1650 (w), 1585 (vs), 1448 (s), 1387 (vs), 1310 (w), 1259 (s), 1214 (w), 1163 (w), 1067 (vs), 1010 (vs), 955 (w), 852 (w), 798 (s), 732 (vw), 617 cm⁻¹ (vw); UV/Vis (toluene): λ (ϵ) = 620 (345), 365 nm (1429 mol⁻¹ dm³ cm⁻¹); MS (ESI): m/z : 781 [Cu₂L₂]⁺, 720 [CuL₂H₂]⁺, 423 [CuL(MeOH)]⁺, 391 [CuL]⁺; elemental analysis calcd (%) for C₃₀H₄₂N₂O₁₄Cu₂ (781.76): C 46.09, H 5.42, N 3.58, Cu 16.3; found C 45.67, H 5.38, N 3.36, Cu 16.1.

Bis[1,2-*O*-isopropylidene-6-*N*-(2,2-bisethylcarboxyethylene)amino-6-deoxyglucufuranosyl]dicopper(II), Cu(3b): The isolation of Cu(3b) was carried out in an analogous manner to that of Cu(3a). Yield: 144 mg (66%); IR (KBr): $\tilde{\nu}$ = 3434 (w), 2980 (s), 2933 (s), 2902 (s), 1738 (w), 1714 (w), 1686 (w), 1653 (vs), 1616 (vs), 1570 (vs), 1503 (w), 1441 (s), 1426 (s), 1376 (s), 1342 (s), 1286 (s), 1212 (s), 1166 (s), 1122 (s), 1064 (vs), 1009 (vs), 847 (s), 803 (w), 785 (w), 732 (w), 677 cm⁻¹ (w); UV/Vis (toluene): λ (ϵ) = 626 (601), 346 nm (3172 mol⁻¹ dm³ cm⁻¹); MS (ESI): m/z : 933 [Cu₂L₂(MeOH)]⁺, 452 [CuL+H]⁺; elemental analysis calcd (%) for C₃₄H₅₀N₂O₁₈Cu₂ (901.86): C 45.28, H 5.59, N 3.11, Cu 14.1; found C 45.47, H 5.48, N 3.21, Cu 14.1%.

Triethylammonium bis[2-*N*-(3-acetylbut-3-en-2-one)amino-2-deoxyglucopyranosyl]- μ -acetato]dicuprate(II), Cu(4a), and triethylammonium bis[2-*N*-(3-ethylcarboxylbut-3-en-2-one)amino-2-deoxyglucopyranosyl]- μ -acetato]dicuprate(II), Cu(4c): 2-Amino-2-deoxyglucopyranose hydrochloride (1 g, 4.64 mmol) was suspended in methanol (10 mL) and triethylamine (1.29 mL, 9.28 mmol) was added. 3-Ethoxymethylene-2,4-pentandione (0.72 g, 4.64 mmol) or 3-ethoxy-2-acetyl-prop-2-ene acid ethyl ester

(0.86 g, 4.64 mmol), respectively, in methanol (10 mL) were added dropwise. The solution was heated under reflux for 1 h, and was then allowed to stand overnight. The ligands were then precipitated by the addition of diethyl ether to yield colorless powders.

Ligand H₂4a (1 g, 3.46 mmol) or H₂4c (1 g, 3.13 mmol) were dissolved in methanol (15 mL) and triethylamine (0.96 mL, 6.92 mmol) or (0.87 mL, 6.26 mmol), respectively, was added. This solution was added dropwise to a suspension of copper(II) acetate monohydrate (0.69 g, 3.46 mmol or 0.62 g, 3.13 mmol, respectively) in methanol (5 mL). The dark blue solution was stirred for 30 minutes. Diethyl ether was added and a blue powder precipitated. This was identified to be pure Cu(4a) or Cu(4c), respectively. Yield: 2.00 g (67%) [Cu(4a)] and 2.09 g (72%) [Cu(4c)].

Cu(4a): IR [KBr (4000–450 cm⁻¹), Nujol (450–50 cm⁻¹): $\tilde{\nu}$ = 3392 (s), 2923 (s), 2700 (m), 1683 (w), 1615 (s), 1570 (s), 1508 (w), 1457 (m), 1392 (s), 1357 (m), 1285 (m), 1099 (m), 1084 (m), 1026 (s), 992 (s), 940 (m), 858 (m), 843 (m), 803 (m), 765 (m), 735 (w), 654 (s), 616 (m), 593 (m), 543 (w), 485 (w), 427 (w), 365 (w), 322 (w), 303 (w), 286 (w), 259 (s), 226 (w), 172 (w), 162 (m), 105 (w), 96 cm⁻¹ (m); UV/Vis (MeOH): λ (ϵ) = 660 (161), 360 nm (879 mol⁻¹ dm³ cm⁻¹); MS (ESI) m/z : 1051 [Cu₃L₃+H]⁺, 803 [Cu₂L₂+HNEt₃]⁺, 723 [Cu₂L₂+Na]⁺, 701 [Cu₂L₂+H]⁺, 383 [CuL(MeOH)+H]⁺, 333 [Cu(L-H₂O+H)]⁺, 102 [HNEt₃]⁺; elemental analysis calcd (%) for C₃₂H₅₃N₃O₁₆Cu₂ (862.87): C 44.54, H 6.19, N 4.87, Cu 14.7%; found C 43.84; H 6.34; N 4.91; Cu 14.8.

Cu(4c): IR [KBr (4000–450 cm⁻¹), Nujol (450–50 cm⁻¹): $\tilde{\nu}$ = 3395 (s), 2979 (vs), 2944 (vs), 2739 (s), 2672 (vs), 2622 (vs), 2605 (s), 2531 (m), 2498 (s), 1691 (s), 1614 (s), 1572 (m), 1476 (s), 1444 (m), 1398 (s), 1365 (m), 1331 (w), 1271 (m), 1186 (w), 1172 (m), 1094 (m), 1071 (s), 1037 (vs), 915 (w), 851 (m), 807 (m), 774 (m), 638 (w), 597 (w), 539 (w), 462 (w), 427 (w), 365 (w), 322 (w), 303 (w), 286 (w), 259 (s), 226 (w), 172 (w), 162 (m), 105 (w), 96 cm⁻¹ (m); UV/Vis (MeOH): λ (ϵ) = 646 (148), 350 nm (2700 mol⁻¹ dm³ cm⁻¹); MS (ESI): m/z : 1545 [Cu₄L₄+Na]⁺, 1165 [Cu₃L₃+Na]⁺, 783 [Cu₂L₂+Na]⁺, 761 [Cu₂L₂+H]⁺, 445 [CuL(MeOH)₂+H]⁺, 413 [CuL(MeOH)+H]⁺, 381 [CuL+H]⁺, 102 [HNEt₃]⁺; elemental analysis calcd (%) for C₃₄H₅₇N₃O₁₈Cu₂ (922.93): C 44.24, H 6.22, N 4.55, Cu 13.7; found C 43.58, H 6.50, N 4.45, Cu 13.6.

3-[*N*-(2-Hydroxycyclohexyl)aminomethylene]-2,4-pentadione (H₂5a): *trans*-Cyclohexanollammonium chloride (3.04 g, 0.02 mol) was suspended in chloroform (20 mL). Triethylamine (4.04 g, 0.04 mol) was added, and the solution was stirred for 30 minutes. 3-Ethoxymethylene-2,4-pentandione (3.12 g, 0.02 mol) in chloroform (10 mL) was added, and the mixture was heated under reflux for 2 h. After cooling, diethyl ether was added to the solution. The triethylammonium chloride precipitate was filtered off. After evaporation of the solvent, the remaining oil was purified by recrystallization from an ethanol/water mixture. Yield: 3.56 g (79%). ¹H NMR (200 MHz, CDCl₃, 25 °C, TMS): δ = 10.94 (dd, 1H; N-H), 8.40 (d, 1H; =CH-), 3.41 (m, 2H; CH₂), 2.97 (m, 2H; CH₂), 2.39 (m, 1H; CH), 2.34 (s, 3H; CH₃), 2.32 (dd, 1H), 2.20 (s, 3H; CH₃), 1.95 (m, 2H; CH₂), 1.78 (m, 2H; CH₂); ¹³C NMR (PENDANT, 200 MHz, CDCl₃, TMS): δ = 199 (quart. C), 195 (quart. C), 160 (CH), 110 (quart. C), 74 (CH), 65 (CH), 46 (CH₂), 34 (CH₂), 31.5 (CH₃), 31 (CH₂), 26 (CH₃), 24 (CH₂); IR (KBr): $\tilde{\nu}$ = 3487 (s), 2982 (s), 2937 (s), 2861 (s), 2757 (m), 2739 (w), 2677 (w), 2603 (w), 2450 (w), 1680 (vs), 1635 (vs), 1583 (s), 1476 (m), 1427 (s), 1388 (s), 1360 (s), 1302 (m), 1258 (s), 1241 (s), 1195 (w), 1142 (m), 1120 (w), 1077 (s), 1021 (m), 975 (m), 953 (w), 939 (w), 865 (m), 822 (s), 764 (m), 724 (w), 590 (m), 549 (m), 474 cm⁻¹ (w); elemental analysis calcd (%) for C₁₂H₁₉N₃O₅ (225.29): C 63.97, H 8.50, N 6.21; found C 63.76, H 8.39, N 6.24.

Tetrakis-[3-[*N*-(2-oxycyclohexyl)aminomethylene]-2,4-pentanedione-(2-*O*’,*N*’,*O*’)tetracopper(II), Cu(5a): Solid copper acetate monohydrate (0.80 g, 4 mmol) was added to H₂5a (0.91 g, 4 mmol) in chloroform (20 mL). After addition of triethylamine (20 drops), the copper salt dissolved and the solution turned deep blue. The solution was allowed to stand in an open round flask for 2 d to yield deep blue crystals. Crystals in quality suitable for X-ray crystal structure analysis were obtained by the addition of pyridine (10 mL) before the solvent was allowed to evaporate. Yield: 0.46 g (36.4%); IR [KBr (4000–450 cm⁻¹), Nujol (450–50 cm⁻¹): $\tilde{\nu}$ = 3433 (m), 3252 (w/sh), 2930 (vs), 2857 (vs), 1735 (w), 1654 (s), 1607 (vs), 1507 (w), 1467 (s), 1400 (vs), 1355 (m), 1275 (s), 1236 (s), 1209 (w), 1179 (w), 1145 (m), 1124 (w), 1081 (m), 1064 (m), 1027 (m), 990 (m), 940 (m), 921 (m), 890 (w), 858 (m), 801 (w), 756 (w), 670 (m), 635 (s), 622 (m), 591 (m), 551 (m), 460 (m), 422 (m), 362 (m), 332 (w), 317 (w), 286 (m), 259 (s), 176 (w/sh), 168,

(m), 96 cm⁻¹ (m); UV/Vis (CHCl₃): λ (ε) = 632 (147), 359 nm (808 mol⁻¹ dm³ cm⁻¹); MS (DEI): m/z: 572 [M/2]⁺, 286 [CuL]⁺; elemental analysis calcd (%) for C₄₈H₆₈N₄O₁₂Cu₄ (1147.27): C 50.25, H 5.97, N 4.88, Cu 22.2; found C 49.84, H 5.73, N 4.86, Cu 22.4.

Ethyl-2-[N-(2-hydroxycyclohexyl)aminomethylene]-3-oxobutanoate (H₂5c): Triethylamine (4.04 g, 0.04 mol) was added to a suspension of *trans*-cyclohexan ammonium chloride (3.04 g, 0.02 mol) in chloroform (20 mL). The solution was stirred for 30 min. Ethyl-(3-ethoxymethylene)acetate (3.72 g, 0.02 mol) in chloroform (10 mL) was added, and the mixture was heated under reflux for 2 h. After cooling, diethyl ether was added to the solution. The triethylammonium chloride precipitate was filtered off. After evaporation of the solvent, the remaining oil was purified by recrystallization from an ethanol/water mixture. Yield: 3.42 g (67%). ¹H NMR (200 MHz, CDCl₃, TMS): δ = 10.86 (dd, 1H; NH), 8.02 (d, 1H; =CH-), 3.34 (dd, 2H; CH₂), 3.28 (m, 1H; CH), 2.84 (dd, 1H; CH), 2.19 (s, 3H; CH₃), 1.93 (dd, 2H; CH₂), 1.68 (dd, 2H; CH₂), 1.30 (m, 7H); ¹³C NMR (PENDANT, 200 MHz, CDCl₃, TMS): δ = 197 (quart.C), 167 (quart.C), 160 (CH), 99 (quart.C), 74 (CH), 65 (CH), 56 (CH₂), 46 (CH₂), 34 (CH₂), 31.5 (CH₃), 31 (CH₂), 24 (CH₂), 14 (CH₃); IR (KBr): ν̄ = 3385 (s), 2938 (s), 2860 (s), 2740 (m), 2676 (s), 2623 (s), 2604 (s), 2530 (s), 2497 (s), 1733 (m), 1699 (m), 1653 (vs), 1613 (vs), 1564 (s), 1506 (m), 1455 (m), 1400 (vs), 1357 (s), 1324 (m), 1309 (s), 1260 (m), 1248 (m), 1226 (m), 1186 (m), 1142 (w), 1129 (m), 1090 (m), 1068 (m), 1035 (m), 1004 (m), 983 (m), 951 (w), 940 (w), 928 (s), 857 (m), 813 (s), 788 (w), 633 (m), 589 (m), 569 (m), 538 (m), 474 cm⁻¹ (m); elemental analysis calcd (%) for C₁₅H₂₁NO₄ (255.31): C 61.16, H 8.29, N 5.49; found C 60.76, H 8.19, N: 5.44.

Tetrakis-[ethyl-2-[N-(2-oxycyclohexyl)aminomethylene]-3-oxobutanoato(2-)-N, O², O³]tetracopper(II), Cu(5c): Solid copper acetate monohydrate (0.80 g, 4 mmol) was added to ligand H₂5c (1.02 g, 4 mmol) in chloroform (20 mL). After addition of triethylamine (20 drops), the copper salt dissolved and the solution turned deep blue. The solution was allowed to stand in an open round flask bottle for 2 d to yield deep blue crystals in quality suitable for X-ray crystal structure analysis. Yield: 0.46 g (36.4%); IR [KBr (4000–450 cm⁻¹), Nujol (450–50 cm⁻¹): ν̄ = 3425 (s), 2977 (s), 2934 (vs), 2856 (s), 2805 (w), 2757 (m), 2739 (m), 2677 (s), 2603 (w), 2492 (m), 1698 (vs), 1673 (s), 1619 (s), 1584 (w), 1472 (s), 1428 (vs), 1396 (m), 1364 (m), 1355 (w), 1336 (w), 1279 (s), 1259 (vs), 1242 (w), 1184 (m), 1145 (m), 1077 (s), 1047 (s), 1038 (m), 1016 (m), 951 (w), 873 (w), 859 (m), 800 (m), 773 (m), 681 (m), 655 (s), 624 (m), 588 (m), 547 (m), 458 (m), 423 (m), 264 (m), 332 (w), 315 (m), 286 (w), 259 (s), 228 (w), 167 (m), 108 (w), 97 cm⁻¹ (w); UV/Vis (CHCl₃): λ (ε) = 629 (171), 356 nm (651 mol⁻¹ dm³ cm⁻¹); MS (DEI): m/z: 632 [Cu₂L₂]⁺, 587, 552, 522, 480, 408, 316 [CuL]⁺, 270, 255 [L]⁺, 184, 138, 105, 60, 43; elemental analysis calcd (%) for C₅₂H₇₆N₄O₁₆Cu₄ (1267.37): C 49.28, H 6.04, N 4.42, Cu 20.1; found C 47.85, H 6.53, N 4.46, Cu 19.9.

X-ray crystallography: Crystallographic data (excluding structure factors) for the structures reported in this paper have been deposited with the Cambridge Crystallographic Data Centre as supplementary publication nos. CCDC-129254, 129253, 138083, and 138084 for Cu(1a), Cu(2a), Cu(5c), and Cu(5a), respectively. Copies of the data can be obtained free of charge on application to CCDC, 12 Union Road, Cambridge CB2 1EZ, UK (fax: (+44)1223-336-033; e-mail: deposit@ccdc.cam.ac.uk).

Acknowledgements

This work was supported by the Deutsche Forschungsgemeinschaft (Sonderforschungsbereich 436 "Metallvermittelte Reaktionen nach dem Vorbild der Natur") and the Fonds der Chemischen Industrie. We thank Dr. M. Friedrich for EPR measurements and Dr. W. Poppitz for mass spectroscopic measurements.

- [1] a) T. Klabunde, C. Eicken, J. C. Sacchettini, B. Krebs, *Nat. Struct. Biol.* **1998**, *5*, 1084–1090; b) A. Rompel, H. Fischer, D. Meiwes, K. Büldt-Karentzopoulos, R. Dillinger, F. Tuzcek, H. Witzel, B. Krebs, *J. Biol. Inorg. Chem.* **1999**, *4*, 56–63.
[2] A. Messerschmidt, *Metal Sites in Proteins and Models* **1998**, *90*, 37–68; A. Messerschmidt, H. Luecke, R. Huber, *J. Mol. Biol.* **1993**, *997*.

- [3] R. Than, A. A. Feldmann, B. Krebs, *Coord. Chem. Rev.* **1999**, *182*, 211–241.
[4] J. Reedijk, *Bioinorganic Catalysis*, (Ed.: J. Reedijk), 2nd ed., Dekker, New York **1998**.
[5] J. Reim, B. Krebs, *J. Chem. Soc. Dalton Trans.* **1997**, 3793–3804.
[6] a) E. Monzani, G. Battaini, A. Perotti, L. Casella, M. Gullotti, L. Santagostini, G. Nardin, L. Randaccio, S. Geremia, P. Zanella, G. Opromella, *Inorg. Chem.* **1999**, *38*, 5359–5369; b) E. Monzani, L. Quinti, A. Perotti, L. Casella, M. Gullotti, L. Randaccio, S. Geremia, G. Nardin, P. Faleschini, G. Tabbi, *Inorg. Chem.* **1998**, *37*, 553; c) L. Casella, E. Monzani, M. Gullotti, D. Cavagnino, G. Cerina, L. Santagostini, R. Ugo, *Inorg. Chem.* **1996**, *35*, 7516–7525.
[7] F. Thaler, C. D. Hubbard, F. W. Heinemann, R. van Eldik, S. Schindler, I. Fabian, A. M. Dittler-Klingemann, F. E. Hahn, C. Orvig, *Inorg. Chem.* **1998**, *37*, 4022–4029.
[8] E.-G. Jäger, in *Chemistry at the Beginning of the Third Millennium* (Eds.: L. Fabbri, A. Poggi), Springer, Berlin-Heidelberg-New York, **2000**, pp. 103–138; b) E.-G. Jäger, J. Knaut, K. Schuhmann, A. Guba, in *Peroxide Chemistry: Mechanistic and Preparative Aspects of Oxygen Transfer*, Wiley-VCH, Weinheim, **2000**, pp. 249–280.
[9] E.-G. Jäger, *Z. Chem.* **1966**, *6*, 111.
[10] a) J. J. Bertrand, J. A. Kelley, C. E. Kirkwood, *Chem. Commun.* **1968**, 1329–1331; b) J. A. Bertrand, J. A. Kelley, *Inorg. Chim. Acta* **1970**, *4*, 203–209.
[11] a) J. A. Bertrand, J. A. Kelley, J. L. Breece, *Inorg. Chim. Acta* **1970**, *4*, 247–250; b) J. A. Bertrand, C. Marabella, D. G. Vanderveer, *Inorg. Chim. Acta* **1978**, *26*, 113–119.
[12] a) E. Sinn, *Inorg. Chem.* **1976**, *15*, 358–365; b) J. A. Davis, E. Sinn, *J. Chem. Soc. Dalton Trans.* **1976**, 165–170.
[13] a) N. Matsumoto, T. Tsutsumi, A. Ohyoshi, H. Okawa, *Bull. Chem. Soc. Jpn.* **1983**, *56*, 1386–1392; b) N. Matsumoto, I. Ueda, Y. Nishida, S. Kida, *Bull. Chem. Soc. Jpn.* **1976**, *49*, 1308–1312; c) N. Matsumoto, T. Kondo, M. Kodera, H. Okawa, S. Kida, *Bull. Chem. Soc. Jpn.* **1989**, *62*, 4041–4043.
[14] F. Wiesemann, B. Krebs, H. Görls, E.-G. Jäger, *Z. anorg. allg. Chem.* **1995**, *621*, 1883–1892.
[15] a) W. Haase, *Chem. Ber.* **1973**, *106*, 3132–3148; b) L. Merz, W. Haase, *J. Chem. Soc. Dalton Trans.* **1978**, 1594–1598; c) L. Merz, W. Haase, *J. Chem. Soc. Dalton Trans.* **1980**, 875–879; d) R. Mergehenn, L. Merz, W. Haase, *J. Chem. Soc. Dalton Trans.* **1980**, 1703–1709; e) L. Walz, H. Paulus, W. Haase, H. Langhof, F. Nepveu, *J. Chem. Soc. Dalton Trans.* **1983**, 657–664; f) L. Schwabe, W. Haase, *J. Chem. Soc. Dalton Trans.* **1985**, 1909–1913; g) H. Astheimer, F. Nepveu, L. Walz, W. Haase, *J. Chem. Soc. Dalton Trans.* **1985**, 315–320.
[16] H. Oshio, Y. Saito, T. Ito, *Angew. Chem.* **1997**, *122*, 2789–2791; *Angew. Chem. Int. Ed. Engl.* **1997**, *36*, 2673–2675.
[17] Yu. M. Chumakov, V. N. Biyushkin, T. I. Malinovskii, S. Kulemu, V. I. Tsapkov, M. S. Popov, N. M. Samus, *Koord. Khim.* **1990**, *16*, 945–949.
[18] a) V. Tangoulis, S. Paschalidou, E. G. Bakalbassis, S. P. Perlepes, C. P. Raptopoulou, A. Terzis, *Chem. Commun.* **1996**, 1297–1298; b) V. Tangoulis, C. P. Raptopoulou, A. Terzis, S. Paschalidou, S. P. Perlepes, E. G. Bakalbassis, *Inorg. Chem.* **1997**, *36*, 3996–4006.
[19] G. A. van Albada, J. Reedijk, R. Hamalainen, U. Turpeinen, A. L. Spek, *Inorg. Chim. Acta* **1989**, *163*, 213–217.
[20] P. L. Dedert, T. Sorrell, T. J. Marks, J. A. Ibers, *Inorg. Chem.* **1982**, *21*, 3506–3517.
[21] a) H. Muhonen, *Acta Chem. Scand. Ser. A* **1980**, *34*, 79; b) H. Muhonen, W. E. Hatfield, J. H. Helms, *Inorg. Chem.* **1986**, *25*, 800–812.
[22] J. Sassmannshausen, H. F. von Schnering, L. Walz, *Z. Kristallogr.* **1997**, *212*, 656–661.
[23] H. Keutel, H. Görls, W. Poppitz, A. Schütz, E.-G. Jäger, *J. Prakt. Chem.* **1999**, *341*, 785–791.
[24] R. Wegner, M. Gottschaldt, H. Görls, E.-G. Jäger, D. Klemm, *Angew. Chem.* **2000**, *125*, 608–612; *Angew. Chem. Int. Ed.* **2000**, *39*, 595–599.
[25] D. Klemm, T. Heinze, B. Philipp, W. Wagenknecht, *Acta Polym.* **1977**, *48*, 277–297.
[26] D. Klemm, B. Philipp, T. Heinze, U. Heinze, W. Wagenknecht, *Comprehensive Cellulose Chemistry, Vols. 1 and 2*, Wiley-VCH, Weinheim, **1998**.
[27] J. Tiller, P. Berlin, D. Klemm, *Macromol. Chem. Phys.* **1999**, *200*, 1–9.
[28] D. N. Williams, U. Piarulli, C. Floriani, A. Chiesi-Villa, C. Rizzoli, *J. Chem. Soc. Dalton Trans.* **1994**, 1243–1250.

- [29] a) P. Klüfers, H. Piotrowski, J. Uhlendorf, *Chem. Eur. J.* **1997**, *3*, 601–608; b) H. P. Wu, C. Janiak, P. Klüfers, P. Mayer, *Chem. Commun.* **1998**, 2637–2638; c) P. Mayer, P. Klüfers, *Acta Crystallogr. Sect. C* **1998**, *54*, 583–586; d) R. Ahlrichs, B. Ballauf, K. Eichkorn, O. Hanemann, G. Kettenbach, P. Klüfers, *Chem. Eur. J.* **1998**, *4*, 835–844; e) A. Geisselmann, P. Klüfers, B. Pilawa, *Angew. Chem.* **1998**, *123*, 1181–1184; *Angew. Chem. Int. Ed.* **1998**, *37*, 1119–1121; f) J. Bürger, P. Klüfers, *Z. Anorg. Allg. Chem.* **1998**, *624*, 359–360.
- [30] a) S. Yano, *Coord. Chem. Rev.* **1988**, *92*, 113–156; b) S. Yano, M. Doi, S. Tamakoshi, W. Mori, M. Mikuriya, A. Ichimura, I. Kinoshita, Y. Yamamoto, T. Tanase, *Chem. Commun.* **1997**, 997–998; c) S. Yano, S. Inoue, R. Nouchi, M. Reiko, S. Kaoru, Y. Yoshie, Y. Yasuda, M. Kato, T. Tanase, T. Kakuchi, Y. Mikata, T. Suzuki, Y. Yamamoto, *J. Inorg. Biochem.* **1998**, *69*, 15–23; d) T. Tanase, T. Onaka, M. Hakagoshi, I. Kinoshita, S. Shibata, M. Doe, J. Fujii, S. Yano, *Chem. Commun.* **1997**, 2115–2116; e) T. Tsubomura, M. Ogawa, S. Yano, K. Kobayashi, T. Sakurai, S. Yoshikawa, *Inorg. Chem.* **1990**, *29*, 2622–2626.
- [31] Zhou, B. Wagner, K. Polborn, K. Sunkel, W. Beck, *Z. Naturforsch. Teil B* **1994**, *49*, 1193–1202.
- [32] J. M. Harrowfield, M. Mocerino, B. W. Skelton, W. Wei, A. H. White, *J. Chem. Soc. Dalton Trans.* **1995**, 783–797.
- [33] a) A. Bernalte-Garcia, M. A. Diaz-Diez, F. J. Garcia-Barros, F. J. Higes-Rolando, C. Valenzuela-Calahorra, *Transition Met. Chem.* **1996**, *21*, 197–199; b) M. A. Diaz-Diez, F. J. Garcia-Barros, F. J. Higes-Rolando, A. Bernalte-Garcia, C. Valenzuela-Calahorra, *Transition Met. Chem.* **1995**, *20*, 402–405; c) M. A. Diaz-Diez, F. J. Garcia-Barros, F. J. Higes-Rolando, A. Bernalte-Garcia, C. Valenzuela-Calahorra, *Polyhedron* **1993**, *12*, 2519–2523.
- [34] a) K. Hegetschweiler, M. Weber, V. Huch, R. J. Geue, A. D. Rae, A. C. Willis, A. M. Sargeson, *Inorg. Chem.* **1998**, *37*, 6136–6146; b) G. J. Reiss, W. Frank, K. Hegetschweiler, D. Kuppert, *Acta Crystallogr. Sect. C* **1998**, *54*, 614–616; c) L. Hausherr-Primo, K. Hegetschweiler, H. Ruegger, L. Odier, R. D. Hancock, H. W. Schmalte, V. Gramlich, *J. Chem. Soc. Dalton Trans.* **1994**, 1689–1701.
- [35] a) M. M. Svaan, T. Anthonen *Acta Chem. Scand. Ser. B* **1986**, *40*, 2, 119–122; b) K. I. Sato, J. Yoshimura, *Carbohydr. Res.* **1982**, *103*, 221–238; c) K. Jones, W. W. Wood, *Carbohydr. Res.* **1986**, *155*, 217–222; d) B. P. Bashyal, H. F. Chow, L. E. Fellows, G. W. J. Fleet, *Tetrahedron* **1987**, *43*, 415–422; e) K. Dax, B. Gaigg, V. Grassberger, B. Kölbinger, A. E. Stütz, *J. Carbohydr. Res.* **1990**, *9*, 479–499; f) C. B. Barlow, R. D. Guthrie, *J. Chem. Soc. C* **1967**, 1194–1196; g) A. Fürstner, J. Baumgartner, D. N. Jumbam, *J. Chem. Soc. Perkin Trans. I* **1993**, *1*, 131–138; h) F. Cramer, H. Otterbach, H. Springmann, *Chem. Ber.* **1959**, *92*, 384–391; i) K. Y. Ko, J. Y. Park, *Tetrahedron Lett.* **1997**, *38*, 3, 407–410.
- [36] O. Kahn, *Molecular Magnetism*, VCH Publishers, New York, **1993**; K. D. Karlin, Y. Gultneh, T. Nicholson, J. Zubieta, *Inorg. Chem.*, **1985**, *24*, 3727.
- [37] N. Oishi, Y. Nishida, K. Ida, S. Kida, *Bull. Chem. Soc. Jpn.* **1980**, *53*, 2847.
- [38] U. Casellato, S. Tamburini, P. A. Vigato, A. de Stefani, M. Vidali, D. E. Fenton, *Inorg. Chim. Acta* **1983**, *69*, 45.
- [39] M. R. Malachowski, M. G. Davidson, *Inorg. Chim. Acta* **1989**, *162*, 199.
- [40] M. R. Malachowski, H. B. Huynh, L. J. Tomlinson, R. S. Kelly, J. W. Furbee, Jr., *J. Chem. Soc. Dalton Trans.* **1995**, 31.
- [41] F. Zippel, F. Ahlers, R. Werner, W. Haase, H.-F. Nolting, B. Krebs, *Inorg. Chem.* **1996**, *35*, 3409–3419.
- [42] M. R. Malachowski, J. Carden, M. G. Davidson, W. L. Driessen, J. Reedijk, *Inorg. Chim. Acta* **1997**, *257*, 59–67.
- [43] Y.-H. Chung, H.-H. Wei, Y.-H. Liu, G.-H. Lee, Y. Wang, *J. Chem. Soc. Dalton Trans.* **1997**, 2825–2829.
- [44] J. Manzur, A. M. Garcia, V. Rivas, A. M. Atria, J. Valenzuela, E. Spodine, *Polyhedron* **1997**, *16*, 2299–2305.
- [45] S. Parimala, K. N. Gita, M. Kandaswamy, *Polyhedron* **1998**, *17*, 3445–3453.
- [46] M. R. Malachowski, B. T. Dorsey, M. J. Parker, M. E. Adams, R. S. Kelly, *Polyhedron* **1998**, *17*, 1289–1294.
- [47] a) K. D. Karlin, M. S. Nasin, B. I. Cohen, R. W. Cruse, S. Kaderli, A. D. Zuberbühler, *J. Am. Chem. Soc.* **1994**, *116*, 1324–1336; b) K. D. Karlin, N. Wei, B. Jung, S. Kaderli, P. Niklaus, A. D. Zuberbühler, *J. Am. Chem. Soc.* **1993**, *115*, 9506–9514.
- [48] G. Battaini, E. Monzani, L. Casella, L. Santagostini, R. Pagliarin, *J. Biol. Inorg. Chem.* **2000**, *5*, 262–268.
- [49] R. Wegner, M. Dubs, H. Görls, E.-G. Jäger, B. Schönecker, unpublished results.
- [50] W. B. Tolman, *Acc. Chem. Res.* **1997**, *30*, 227–237.
- [51] P. L. Holland, W. B. Tolman, *Coord. Chem. Rev.* **1990**, *190–192*, 855–869.
- [52] K. D. Karlin, D.-H. Lee, H. V. Obias, K. J. Humphreys, *Pure Appl. Chem.* **1998**, *70*, 855–862.

Received: March 29, 2000

Revised version: January 3, 2001 [F2392]